

Synthesis and Structure–Activity Correlation of Natural-Product Inspired Cyclodepsipeptides Stabilizing F-Actin

René Tannert, Lech-Gustav Milroy, Bernhard Ellinger, Tai-Shan Hu, Hans-Dieter Arndt,* and Herbert Waldmann*

Max-Planck-Institut für molekulare Physiologie, Otto-Hahn-Strasse 11, 44227 Dortmund, Germany, and Technische Universität Dortmund Fakultät Chemie, Otto-Hahn-Strasse 6, 44221 Dortmund, Germany

Received November 9, 2009; E-mail: hans-dieter.arndt@mpi-dortmund.mpg.de; herbert.waldmann@mpi-dortmund.mpg.de

Abstract: The fundamental role played by actin in the regulation of eukaryotic cell maintenance and motility renders it a primary target for small-molecule intervention. In this arena, a class of potent cytotoxic cyclodepsipeptide natural products has emerged over the last quarter-century to stimulate the fields of biology and chemistry with their unique actin-stabilizing properties and complex peptide–polyketide hybrid structures. Despite considerable research effort, a structural basis for the activity of these secondary metabolites remains elusive, not least for the lack of high-resolution structural data and a reliable synthetic route to diverse compound libraries. In response to this, an efficient solid-phase approach has been developed and successfully applied to the total synthesis of jasplakinolide and chondramide C and diverse analogues. The key macrocyclization step was realized using ruthenium-catalyzed ring-closing metathesis (RCM) that in the course of a library synthesis produced discernible trends in metathesis reactivity and *E/Z*-selectivity. After optimization, the RCM step could be operated under mild conditions, a result that promises to facilitate the synthesis of more extensive analogue libraries for structure–function studies. The growth inhibitory effects of the synthesized compounds were quantified and structure–activity correlations established which appear to be in good alignment with relevant biological data from natural products. In this way a number of potent unnatural and simplified analogues have been found. Furthermore, potentially important stereochemical and structural components of a common pharmacophore have been identified and rationalized using molecular modeling. These data will guide in-depth mode-of-action studies, especially into the relationship between the cytotoxicity of these compounds and their actin-perturbing properties, and should inform the future design of simplified and functionalized actin stabilizers as well.

Introduction

In all eukaryotic cells, the tightly regulated assembly and disassembly of actin fibers is fundamental to cellular growth and dynamics, and crucial for cell motility and shape maintenance, phagocytosis, and cytokinesis.¹ As such, the potent and selective perturbation of actin-mediated processes by means of small molecules carries considerable therapeutic potential. In nature, functionally distinct actin-modulator compounds have been found that act according to their ability to either (a) disrupt actin filament assembly, (b) induce actin polymerization and stabilize actin fibers, or (c) inhibit actin-binding proteins that control processes such as actin polymer nucleation.² These natural products have been important tools for the study of actin structure and function,^{2c,d} as well as actin-mediated signal

transduction events,³ and represent promising leads for the development of new cancer⁴ and malaria⁵ chemotherapies. Moreover, actin-targeting small molecules serve as privileged scaffolds that fundamentally address biomacromolecular interactions, as protein–protein interactions dominate the assembly and regulation of actin.⁶

The bicyclic heptapeptide phalloidin (Figure 1, **1**)⁷ was the first natural product shown to stabilize F-actin fibers.⁸ Fluorescent conjugates of **1** are routinely microinjected into cells for the localization of actin fibers,⁹ but weak cell permeability limits its use in the study of live cells and its pursuit as a drug lead. More recently, however, a class of cyclodepsipeptides has

- (1) (a) Disanza, A.; Steffen, A.; Hertzog, M.; Frittoli, E.; Rottner, K.; Scita, G. *Cell. Mol. Life Sci.* **2005**, *62*, 955. (b) Schmidt, A.; Hall, M. N. *Annu. Rev. Cell Dev. Biol.* **1998**, *14*, 305.
- (2) (a) Allingham, J. S.; Klenchin, V. A.; Rayment, I. *Cell. Mol. Life Sci.* **2006**, *63*, 2119. (b) Fenteany, G.; Zhu, S. T. *Curr. Top. Med. Chem.* **2003**, *3*, 593. (c) Peterson, J. R.; Mitchison, T. J. *Chem. Biol.* **2002**, *9*, 1275. (d) Spector, I.; Braet, F.; Shochet, N. R.; Bubb, M. R. *Microsc. Res. Tech.* **1999**, *47*, 18.

- (3) Kustermans, G.; Piette, J.; Legrand-Poels, S. *Biochem. Pharmacol.* **2008**, *76*, 1310.
- (4) (a) Jordan, M. A.; Wilson, L. *Curr. Opin. Cell Biol.* **1998**, *10*, 123. (b) Rao, J. Y.; Li, N. *Curr. Cancer Drug Targets* **2004**, *4*, 345.
- (5) Fotie, J.; Morgan, R. E. *Mini Rev. Med. Chem.* **2008**, *8*, 1088.
- (6) For an example of parallel small-molecule and RNA interference screening leading to the discovery of novel cytokinesis inhibitors, see: Eggert, U. S.; Kiger, A. A.; Richter, C.; Perlman, Z. E.; Perrimon, N.; Mitchison, T. J.; Field, C. M. *PLoS Biol.* **2004**, *2*, e379.
- (7) Wieland, T. *Science* **1968**, *159*, 946.
- (8) Lengsfeld, A. M.; Löw, I.; Wieland, T.; Dancker, P.; Hasselbach, W. *Proc. Natl. Acad. Sci. U.S.A.* **1974**, *71*, 2803.

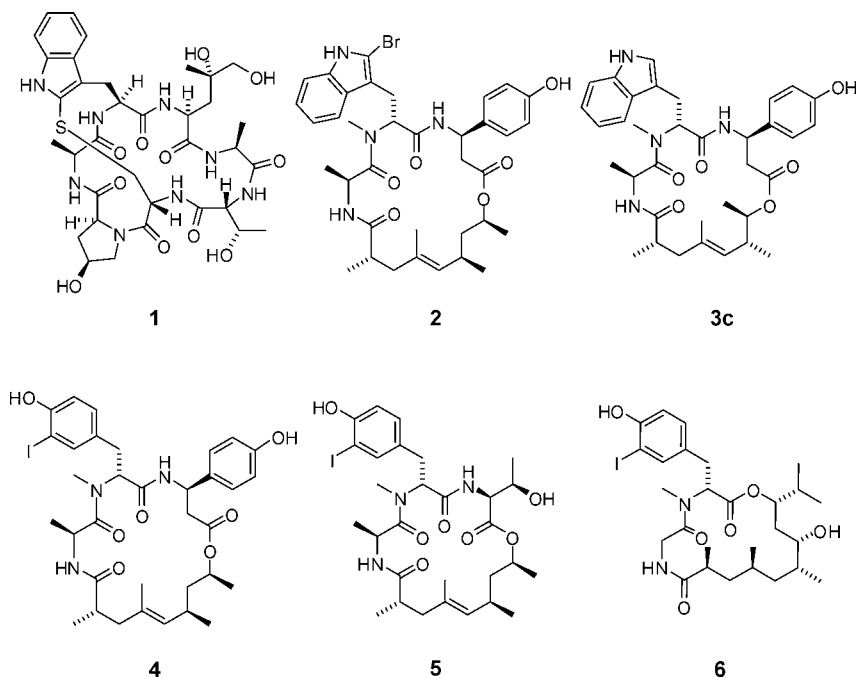


Figure 1. Phalloidin (**1**), jaspalakinolide/jaspamide (**2**), chondramide C (**3c**), geodiamolide H (**4**), seragamide A (**5**), and dolicolide (**6**).

emerged (Figure 1, **2–6**) which competes with phalloidin. In addition to their ability to potently stabilize actin fibers in a manner comparable with **1**, these structurally unique secondary metabolites are also freely cell permeable to render them exciting targets for drug development.

The 19-membered cyclodepsipeptide, jaspalakinolide (Figure 1, **2**),¹⁰ isolated from the marine sponge *Jaspis splendans* in 1986 was the first example and has consequently received the most attention. Isolated independently as “jaspamide”,¹¹ **2** has found widespread use in cell biology research as a cell-permeable probe of actin dynamics.³ Jaspalakinolide competes *in vitro* with **1** for binding to F-actin and stabilizes actin filaments *in vivo*,¹² leading to actin lump formation and polynucleation.^{13a} Furthermore, **2** has shown potent cytotoxicity toward various cancer cell lines,¹³ in addition to its fungicidal,^{10a,14} insecticidal,^{14a} anthelmintic,^{10a,15} ichthyotoxic,¹⁶ herbicidal,^{14a}

and antimalarial activity.¹⁷ More recently, the 18-membered chondramide C (Figure 1, **3c**), isolated from strains of the myxobacterium *Chondromyces crocatus*,¹⁸ was found to potently induce actin polymerization similar to **2**,¹⁹ in addition to its potent antiproliferative activity toward various mammalian cancer cell lines.^{18,20} The geodiamolide (for example, geodiamolide H, **4**, Figure 1)^{10c,21,22} and seragamide families (for example, seragamide A, **5**, Figure 1),²³ and dolicolide (Figure 1, **6**),^{24,25} are further examples of this natural product class. The structural similarity of **2–6** motivates the search for a unifying structural basis for their activity,²⁵ which would be of substantial benefit in the design of new small-molecule probes and more

- (9) (a) Wulf, E.; Deboben, B.; Bautz, F. A.; Faulstich, H.; Wieland, T. *Proc. Natl. Acad. Sci. U.S.A.* **1979**, *76*, 4498. (b) Cooper, J. A. *J. Cell Biol.* **1987**, *105*, 1473.
- (10) Isolation of jaspalakinolide: (a) Crews, P.; Manes, L. V.; Boehler, M. *Tetrahedron Lett.* **1986**, *27*, 2797. See also: (b) Crews, P.; Farias, J. J.; Emrich, R.; Keifer, P. A. *J. Org. Chem.* **1994**, *59*, 2932. (c) Talpir, R.; Benayahu, Y.; Kashman, Y.; Pannell, L.; Schleyer, M. *Tetrahedron Lett.* **1994**, *35*, 4453.
- (11) Isolation of jaspamide: (a) Zabriskie, T. M.; Klocke, J. A.; Ireland, C. M.; Marcus, A. H.; Molinski, T. F.; Faulkner, D. J.; Xu, C.; Clardy, J. *J. Am. Chem. Soc.* **1986**, *108*, 3123. See also: (b) Chevallier, C.; Richardson, A. D.; Edler, M. C.; Hamel, E.; Harper, M. K.; Ireland, C. M. *Org. Lett.* **2003**, *5*, 3737.
- (12) Bubb, M. R.; Senderowicz, A. M. J.; Sausville, E. A.; Duncan, K. L. K.; Korn, E. D. *J. Biol. Chem.* **1994**, *269*, 14869.
- (13) (a) Senderowicz, A. M. J.; Kaur, G.; Sainz, E.; Laing, C.; Inman, W. D.; Rodriguez, J.; Crews, P.; Malspeis, L.; Grever, M. R.; Sausville, E. A.; Duncan, K. L. K. *J. Natl. Cancer I.* **1995**, *87*, 46. (b) Stingl, J.; Andersen, R. J.; Emerman, J. T. *Cancer Chemother. Pharmacol.* **1992**, *30*, 401.
- (14) (a) Peng, J.; Shen, X.; El Sayed, K. A.; Dunbar, D. C.; Perry, T. L.; Wilkins, S. P.; Hamann, M. T.; Bobzin, S.; Huesing, J.; Camp, R.; Prinsen, M.; Krupa, D.; Wideman, M. A. *J. Agric. Food Chem.* **2003**, *51*, 2246. (b) Scott, V. R.; Boehme, R.; Matthews, T. R. *Antimicrob. Agents Chemother.* **1988**, *32*, 1154.
- (15) Crews, P.; Hunter, L. M. *Mar. Biotechnol.* **1993**, *1*, 343.

- (16) Braekman, J. C.; Daloze, D.; Moussiaux, B.; Riccio, R. *J. Nat. Prod.* **1987**, *50*, 994.
- (17) Mizuno, Y.; Makioka, A.; Kawazu, S.; Kano, S.; Kawai, S.; Akaki, M.; Aikawa, M.; Ohtomo, H. *Parasitol. Res.* **2002**, *88*, 844.
- (18) Kunze, B.; Jansen, R.; Sasse, F.; Höfle, G.; Reichenbach, H. *J. Antibiot.* **1995**, *48*, 1262.
- (19) (a) Waldmann, H.; Hu, T.-S.; Renner, S.; Menninger, S.; Tannert, R.; Oda, T.; Arndt, H.-D. *Angew. Chem.* **2008**, *120*, 6573. *Angew. Chem., Int. Ed.* **2008**, *47*, 6473. (b) Eggert, U.; Diestel, R.; Sasse, F.; Jansen, R.; Kunze, B.; Kalesse, M. *Angew. Chem.* **2008**, *120*, 6578. *Angew. Chem., Int. Ed.* **2008**, *47*, 6478.
- (20) Sasse, F.; Kunze, B.; Gronewold, T. M. A.; Reichenbach, H. *J. Natl. Cancer Inst.* **1998**, *90*, 1559.
- (21) (a) Coleman, J. E.; Dilip de Silva, E.; Kong, F.; Andersen, R. J.; Allen, T. M. *Tetrahedron* **1995**, *51*, 10653. (b) Coleman, J. E.; Van Soest, R.; Andersen, R. J. *J. Nat. Prod.* **1999**, *62*, 1137. (c) Chan, W. R.; Tinto, W. F.; Manchard, P. S.; Todaro, L. J. *J. Org. Chem.* **1987**, *52*, 3091. (d) Tinto, W. F.; Lough, A. J.; McLean, S.; Reynolds, W. F.; Yu, M.; Chan, W. R. *Tetrahedron* **1998**, *54*, 4451. (e) Dilip de Silva, E.; Anderson, R. J.; Allen, T. M. *Tetrahedron Lett.* **1990**, *31*, 489.
- (22) (a) Rangel, M.; Prado, M. P.; Konno, K.; Naoki, H.; Freitas, J. C.; Machado-Santelli, G. M. *Peptides* **2006**, *27*, 2047. (b) Freitas, V. M.; Rangel, M.; Bisson, L. F.; Jaeger, R. G.; Machado-Santelli, G. M. *J. Cell Physiol.* **2008**, *216*, 583.
- (23) Tanaka, C.; Tanaka, J.; Bolland, R. F.; Marriott, G.; Higa, T. *Tetrahedron* **2006**, *62*, 3536.
- (24) (a) Ishiwata, H.; Nemoto, T.; Ojika, M.; Yamada, K. *J. Org. Chem.* **1994**, *59*, 4710. (b) Ishiwata, H.; Sone, H.; Kigoshi, H.; Yamada, K. *J. Org. Chem.* **1994**, *59*, 4712. (c) Ishiwata, H.; Sone, H.; Kigoshi, H.; Yamada, K. *Tetrahedron* **1994**, *50*, 12853.
- (25) Bai, R.; Covell, D. G.; Liu, C.; Ghosh, A. K.; Hamel, E. *J. Biol. Chem.* **2002**, *277*, 32165.

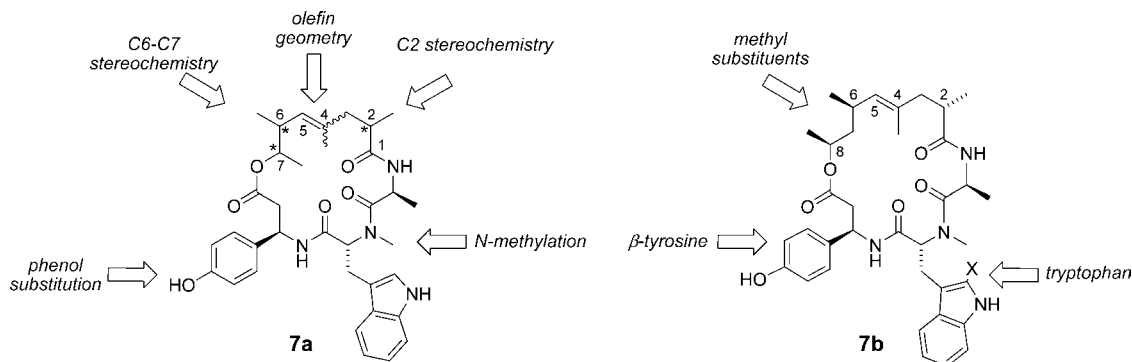


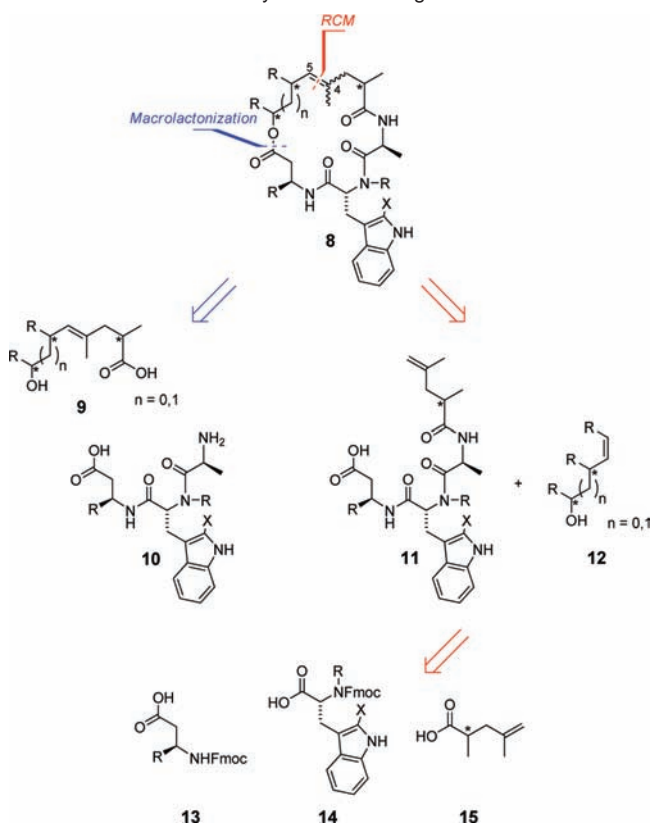
Figure 2. Design of chondramide C (**7a**) and jasplakinolide/jasplamide analogues (**7b**).

efficacious and synthetically accessible actin-targeting drugs.²⁶ Progress toward this desirable goal, however, is severely hampered by the lack of high-resolution crystal structure data^{19a,27} and, not least, by flexible synthetic routes to access diverse structural analogues.

To facilitate investigations into the common molecular parameters of these natural product lead scaffolds,²⁸ we sought to develop a new and efficient synthesis of **2** and **3c** that in extension could be suited to the synthesis of focused sets of analogues. In particular, we intended on studying the relationship between structure and biological activity, initially in terms of macrocycle configuration, through the synthesis and biological evaluation of stereochemically diverse analogues of **3c** (Figure 2, **7a**). The polyketide region had been surmised to ‘program’ the peptide domain into the biologically active conformation.²⁹ We^{19a} and Kalesse and co-workers^{19b} have since realized successful total syntheses of **3c**, which permitted firm stereochemical assignment of the macrocycle scaffold. Here, we sought to scrutinize the crosstalk between polyketide stereochemistry and bioactivity by preparing an extensive collection of stereochemically diverse polyketide analogues of **3c** in search of other biologically active macrocycle configurations. Interestingly, for stereochemically diverse actin-targeting analogues of bistramide A, improved target potency could be shown while our work was ongoing.³⁰

Furthermore, we sought to quantify the significance of structural features found recurrently in this class of cyclodepsipeptide by evaluating a series of strategically simplified analogues inspired by **2**. As we had found jasplakinolide to be quite resistant to major structural simplification,³¹ in line with other research groups,^{29,32,33} we adopted a systematic approach (Figure 2, **7b**). On the basis of our binding hypothesis for **3c**,^{19a} we focused our attention on modifying the β-tyrosine and tryptophan units—both believed to make important contributions to binding to the actin trimer. A desirable outcome of this project

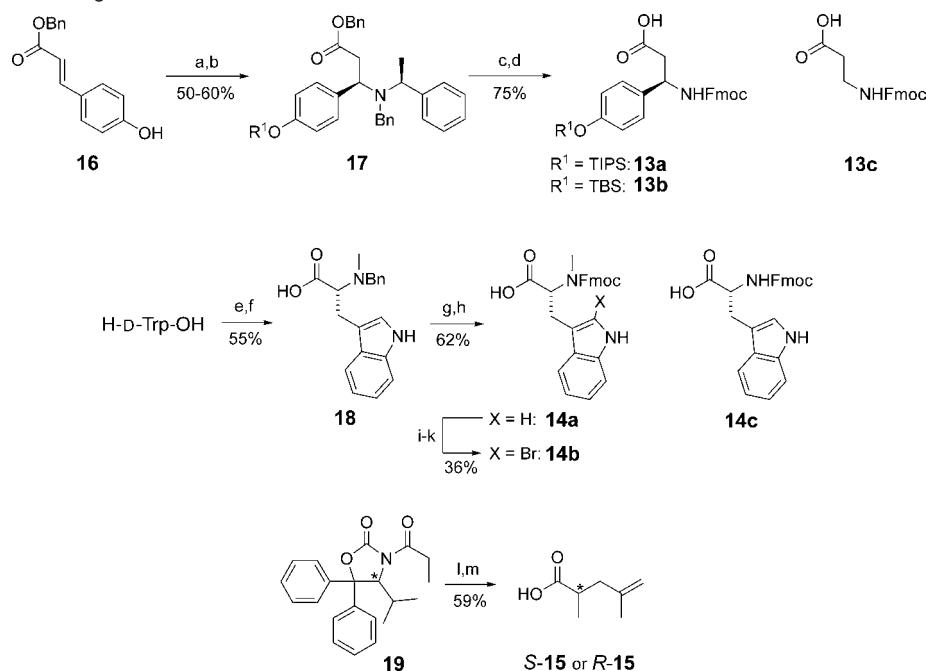
Scheme 1. General Retrosynthetic Planning



was the identification of potent simplified polyketide analogues of **2**. For this reason and for their potential ease of synthesis (commercially available building blocks - *vide infra*), analogues lacking polyketide-based C6- and C8-methyl groups were to be investigated (Figure 2, **7b**). These single-site modifications were expected to increase macrocycle flexibility through the loss of 1,3-allylic and *syn*-pentane interactions²⁹ and hence enable us to test to what extent expected conformational preferences in this region of the molecule impact on biological activity. Here we provide a full account of the synthesis of these molecules along with cytotoxicity and immunostaining studies. We report results from a structure–function analysis of the analogues that is in line with literature data previously reported for other natural products

(26) Newman, D. J.; Cragg, G. M. *J. Nat. Prod.* **2004**, *67*, 1216.
 (27) Recently, the ligand-free F-actin structure was refined to a resolution of 3.3 Å radial and 5.6 Å equatorial: Oda, T.; Iwasa, M.; Aihara, T.; Maeda, Y.; Narita, A. *Nature* **2009**, *457*, 441.
 (28) Kumar, K.; Waldmann, H. *Angew. Chem.* **2009**, *121*, 3272. *Angew. Chem., Int. Ed.* **2009**, *48*, 3224.
 (29) (a) Marimnganti, S.; Yasmeen, S.; Fischer, D.; Maier, M. E. *Chem.–Eur. J.* **2005**, *11*, 6687. (b) Marimnganti, S.; Wieneke, R.; Geyer, A.; Maier, M. E. *Eur. J. Org. Chem.* **2007**, 2779.
 (30) Wrona, I. E.; Lowe, J. T.; Turbyville, T. J.; Johnson, T. R.; Beignet, J.; Beutler, J. A.; Panek, J. S. *J. Org. Chem.* **2009**, *74*, 1897.
 (31) For the synthesis of simplified triazole-derived jasplakinolide analogues, see: Hu, T.-S.; Tannert, R.; Arndt, H.-D.; Waldmann, H. *Chem. Commun.* **2007**, 3942; in biological tests, these compounds were inactive.

(32) Kahn, M.; Nakanishi, H.; Su, T.; Lee, J. Y. H.; Johnson, M. E. *Int. J. Pept. Protein Res.* **1991**, *38*, 324.

Scheme 2. Synthesis of Building Blocks^a

^a Reagents and conditions: (a) TIPSCl or TBSCl, imidazole, DMF, 0 °C → rt, 3 h; (b) (*S*)-*N*-(1-phenylethyl)benzylamine, *n*BuLi, THF, −78 °C, 20–30 min; (c) H₂ (10 bar), Pd(OH)₂/C, AcOH/EtOH, rt, 23 h; (d) NaHCO₃, FmocOSu, 1,4-dioxane/H₂O, 0 °C → rt, 3 h; (e) benzaldehyde, MeOH, rt, 2 h, then NaCNBH₃, 0 °C → rt, 15 h; (f) NaCNBH₃, MeOH, rt, then (CH₂O)_{*n*}, 0 °C, 24 h; (g) H₂ (8 bar), Pd(OH)₂/C, AcOH/EtOH, rt, 20 h; (h) NaOH, NaHCO₃, FmocOSu, 1,4-dioxane/H₂O, 0 °C → rt, 3 h; (i) MeOH, EDC·HCl, (*i*Pr)₂NEt, DMAP, CH₂Cl₂, rt, 17 h; (j) NBS, CH₂Cl₂, rt, 10 min; (k) Me₃SnOH (10 equiv), 1,2-dichloroethane, 80 °C, 20 h; (l) LDA, ZnBr₂, THF, −78 °C, 30 min, then β-methylallyl bromide, −78 °C → −15 °C, 14 h; (m) NaOH, THF/MeOH/H₂O, rt, 2.5 h.

from the same family and are able to align the observed trends with a computationally derived binding mode.

Results and Discussion

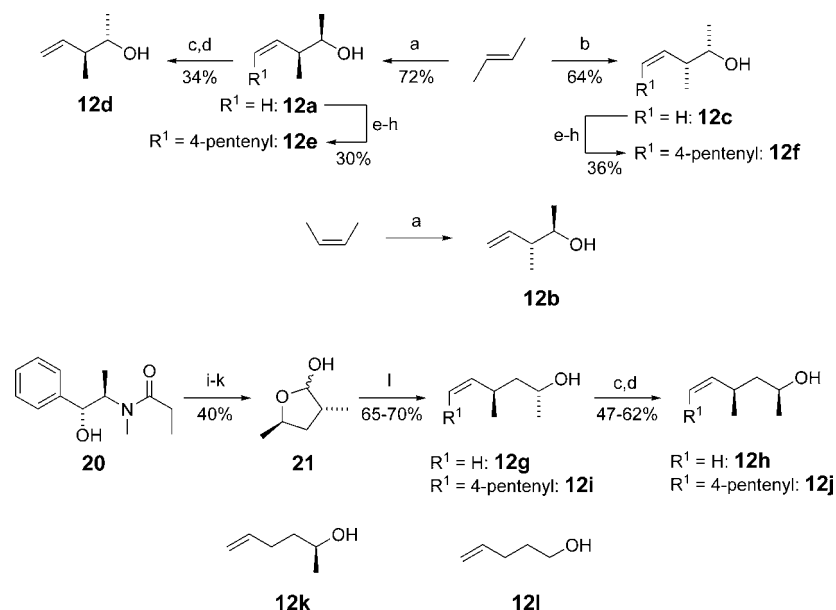
Chemical Synthesis. Retrosynthetic Planning. Jasplakinolide (**2**) has previously been prepared by other research groups using macrolactonization-centered strategies (Scheme 1, **8** → **9** and **10**).³⁴ Concurrent to our efforts,^{19a} chondramide C (**3c**) was prepared using a similar approach.^{19b} In our synthesis design, we opted instead for a novel disconnection across C4–C5 (Scheme 1, **8**) that was anticipated to benefit analogue studies by enabling greater divergence in the polyketide region of the macrocycle at the later stages of the synthesis. This strategy was especially important considering the initial uncertainty surrounding the absolute configuration of **3c**—especially in the polyketide region of the molecule—although biosynthetic considerations³⁵ and the striking similarity between **3c** and **2** left

only the configurations at the C6 and C7 positions in significant doubt (Figure 2, **7a**). Therefore, on the basis of substantial literature precedent for the preparation of cyclopeptides using ring closing metathesis (RCM),³⁶ it was envisaged that the trisubstituted olefin (**8**, Scheme 1) could be formed in a similar manner. In principle, the linear chain could then be simplified to alcohol **12** and peptide acid **11**, which in turn could be disconnected into readily available building blocks **13**–**15** for solid-phase synthesis.

Preparation of Metathesis Precursors. Silyl-protected Fmoc-βTyr-OH (Scheme 2, **13a,b**) was synthesized by capitalizing on the efficient procedure developed by Kocienski for the preparation of H-βTyr(OTBS)-OMe.^{34e} First, silyl-protection of the commercially available benzyl cumarate (**16**) was then followed by stereoselective Michael addition of a chiral benzylic amide to yield amine **17**.³⁷ Hydrogenolysis and subsequent Fmoc-protection yielded acids **13a** and **b** in a reliable 38–45% yield over four steps. The synthesis of Fmoc-D-abrines **14a** and **b** (Scheme 2) was initiated by sequential reductive aminations of D-tryptophan in the presence of the free carboxylic acid group to give *N*-benzyl-abrine (**18**).³⁸ Hydrogenation and Fmoc-protection then yielded Fmoc-abrine (**14a**) in 62% over two steps. For C2-bromination of the indole ring (**14b**), intermediate

- (33) (a) Terracciano, S.; Bruno, I.; Bifulco, G.; Copper, J. E.; Smith, C. D.; Gomez-Paloma, L.; Riccio, R. *J. Nat. Prod.* **2004**, *67*, 1325. (b) Terracciano, S.; Bruno, I.; Bifulco, G.; Avallone, E.; Smith, C. D.; Gomez-Paloma, L.; Riccio, R. *Bioorg. Med. Chem.* **2005**, *13*, 5225. (c) Terracciano, S.; Bruno, I.; D'Amico, E.; Bifulco, G.; Zampella, A.; Sepe, V.; Smith, C. D.; Riccio, R. *Bioorg. Med. Chem.* **2008**, *16*, 6580.
- (34) (a) Grieco, P. A.; Hon, Y. S.; Perez-Medrano, A. *J. Am. Chem. Soc.* **1988**, *110*, 1630. (b) Chu, K. S.; Negrete, G. R.; Konopelski, J. P. *J. Org. Chem.* **1991**, *56*, 5196. (c) Hirai, Y.; Yokota, K.; Momose, T. *Heterocycles* **1994**, *39*, 603. (d) Imaeda, T.; Hamada, Y.; Shioiri, T. *Tetrahedron Lett.* **1994**, *35*, 591. (e) Ashworth, P.; Broadbelt, B.; Jankowski, P.; Kocienski, P.; Pimm, A.; Bell, R. *Synthesis* **1995**, 199. (f) Ghosh, A. K.; Moon, D. K. *Org. Lett.* **2007**, *9*, 2425. See also: (g) Schmid, U.; Siegel, W.; Mundinger, K. *Tetrahedron Lett.* **1988**, *29*, 1269.
- (35) (a) Bai, R. L.; Covell, D. G.; Liu, C. F.; Ghosh, A. K.; Hamel, E. *J. Biol. Chem.* **2002**, *277*, 32165. (b) Rachid, S.; Krug, D.; Weissman, K. J.; Müller, R. *J. Biol. Chem.* **2007**, *282*, 21810.

- (36) (a) Clark, T. D.; Ghadiri, M. R. *J. Am. Chem. Soc.* **1995**, *117*, 12364. (b) Miller, S. J.; Blackwell, H. E.; Grubbs, R. H. *J. Am. Chem. Soc.* **1996**, *118*, 9606. (c) Blackwell, H. E.; Grubbs, R. H. *Angew. Chem.* **1998**, *110*, 3469. *Angew. Chem., Int. Ed.* **1998**, *37*, 3281. (d) Schafmeister, C. E.; Po, J.; Verdine, G. L. *J. Am. Chem. Soc.* **2000**, *122*, 5891. (e) Chapman, R. N.; Dimartino, G.; Arora, P. S. *J. Am. Chem. Soc.* **2004**, *126*, 12252.
- (37) (a) Davies, S. G.; Ichihara, O. *Tetrahedron Asym.* **1991**, *2*, 183. (b) Davies, S. G.; Garrido, N. M.; Kruchinin, D.; Ichihara, O.; Kotchie, L. J.; Price, P. D.; Mortimer, A. J. P.; Russell, A. J.; Smith, A. D. *Tetrahedron: Asymmetry* **2006**, *17*, 1793.

Scheme 3. Synthesis of Alkenes^a

^a Reagents and conditions: (a) KO^tBu, *n*BuLi, THF, $-45\text{ }^{\circ}\text{C}$, 20 min, then (–)-*B*-methoxydiisopinocampheylborane, $-45\text{ }^{\circ}\text{C}$, 30 min, $\text{BF}_3 \cdot \text{Et}_2\text{O}$, CH_3CHO , $-78\text{ }^{\circ}\text{C}$, 4.5 h, then aq NaOH/H₂O₂, reflux, 1 h, 72%; (b) as for (a) using instead (+)-*B*-methoxydiisopinocampheylborane, 64%; (c) *p*-nitrobenzoic acid, PPh₃, DIAD, THF, $0\text{ }^{\circ}\text{C}$, 19 h; (d) NaOH, THF/MeOH/H₂O, $0\text{ }^{\circ}\text{C}$, 15 h; (e) TBSOTf, 2,6-lutidine, CH_2Cl_2 , $-30 \rightarrow -10\text{ }^{\circ}\text{C}$, 40 min (68% starting from **12a**); (f) O₃, CH_2Cl_2 , $-78\text{ }^{\circ}\text{C}$, 5 min; (g) 5-hexenyltriphenylphosphonium iodide, *n*BuLi, THF, $-78\text{ }^{\circ}\text{C}$, 1 h, then add aldehyde, $-78\text{ }^{\circ}\text{C}$, 2 h, 34% (starting from **12a**) or 49% (starting from **12c**), three steps, single isomer (exclusively *Z*-olefin); (h) CSA, MeOH/THF, $0\text{ }^{\circ}\text{C} \rightarrow \text{rt}$, 3 h (88%, **12e**; 30%, four steps), or TBAF, THF, $0\text{ }^{\circ}\text{C} \rightarrow \text{rt}$, 24 h (73%, **12f**; 36%, four steps); (i) LDA, LiCl, THF, $-78\text{ }^{\circ}\text{C}$, then (*R*)-propylene oxide, $0\text{ }^{\circ}\text{C}$, 3.5 h, 86% *d.e.*, (j) aq H₂SO₄ in 1,4-dioxane, rt, then reflux, 90 min; (k) DIBAL-H, CH_2Cl_2 , $-78\text{ }^{\circ}\text{C}$, 1 h; (l) methyltriphenylphosphonium iodide, *n*BuLi, THF or 5-hexenyltriphenylphosphonium iodide, *n*BuLi, THF, $-78\text{ }^{\circ}\text{C}$, 1 h, then add **21**, 2 h, $-78\text{ }^{\circ}\text{C}$, then 2 h, $0\text{ }^{\circ}\text{C}$ (in the case of **12i**, exclusively *Z*-olefin).

protection of the acid function was necessary for reliable yields (Scheme 2, conditions i–k).^{34e} The synthesis of the (*R*)- and (*S*)-enantiomers of pentenoic acid **15** was achieved through the asymmetric α -alkylation of the propanoylated derivative of Seebach's oxazolidinone (**19**)³⁹ with methallyl bromide followed by basic hydrolysis (Scheme 2). X-ray-crystallography unambiguously confirmed the configuration at the C2-position.⁴⁰

For the synthesis of chondramide C (**3c**) and its stereochemical analogues, Brown's crotylboration methodology⁴¹ provided us with convenient one-step access to three of the four C6–C7 homoallylic alcohol diastereomers **12a–c** starting from either *cis*- or *trans*-butene (Scheme 3). Isomer **12d** was most conveniently prepared by Mitsunobu inversion at the C7-position of **12a** followed by saponification (Scheme 3). Toward the synthesis of **2** and simplified analogues, alcohols **12g–j** were synthesized using Myers' pseudoephedrine methodology (Scheme 3).⁴² The lithium enolate derived from pseudoephedrine derivative **20** was alkylated with (*R*)-propylene oxide in the diastereoselectively "matched" sense in good diastereomeric excess (86% *d.e.*), followed by acid-mediated cleavage of the auxiliary and reduction of the intermediate lactone to deliver lactol **21**. At this juncture, Wittig olefination using methyltriphenylphosphonium iodide (**12g**) and Mitsunobu inversion produced alcohol **12h** in the correct configuration for the synthesis of **2**. To bolster our strategic options for RCM studies (*vide infra*), the elaborate dienes **12e,f** were synthesized using a sequence of alcohol

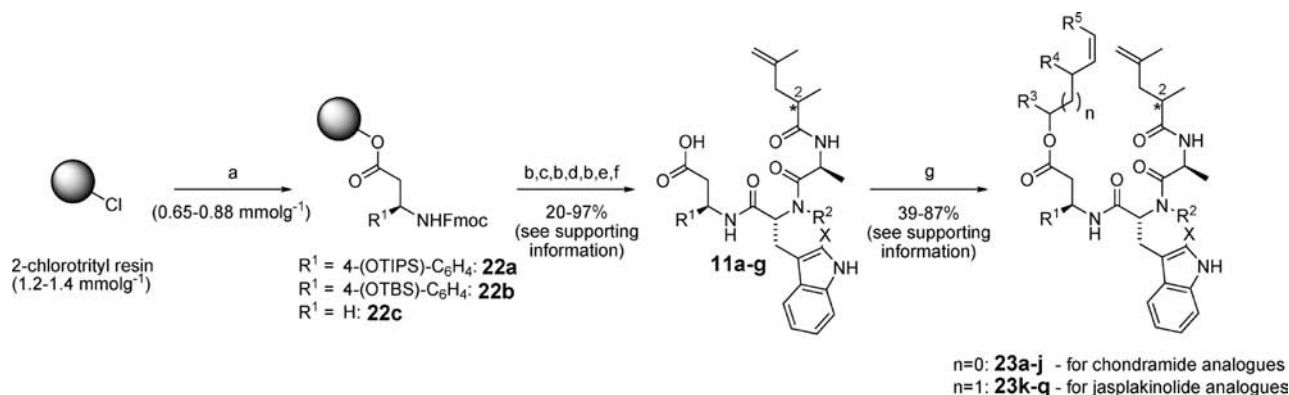
protection, ozonolysis, and Wittig olefination steps (Scheme 3), and **12j** by first reacting 5-hexenyltriphenylphosphonium iodide with lactol **21** to form **12i**, followed by Mitsunobu inversion. In each case, the *Z*-olefin was exclusively detected. The less complex alcohols **12k** and **12l** were commercially available.

With the synthetic building blocks in hand, diverse peptide acids were assembled using Fmoc-based solid-phase peptide synthesis. Silyl-protected Fmoc- β Tyr-OH **13a,b** or Fmoc- β Ala-OH **13c** were first attached to 2-chlorotrityl resin under basic conditions (Scheme 4, **22a–c**). Sequential basic deprotection and carbodiimide-mediated couplings of Fmoc-Trp-OH **14a–c**, Fmoc-Ala-OH, and (*S*)- or (*R*)-pentenoic acid (**15a** or **15b**) followed to yield a variety of peptide acids **11a–g** after resin cleavage (see Supporting Information for structures).⁴³ The esterification of the acid was found to be non-trivial. Standard Mitsunobu conditions⁴⁴ were ineffective. Fortunately, Steglich esterification proved to be highly effective and quite general (Scheme 4) as evidenced by the successful coupling of alcohols **12a–f** for chondramide C analogues ($n = 0$) and **12 h–l** for jasplakinolide analogues ($n = 1$) to afford structurally diverse peptide dienes **23a–q** in moderate to good yields.

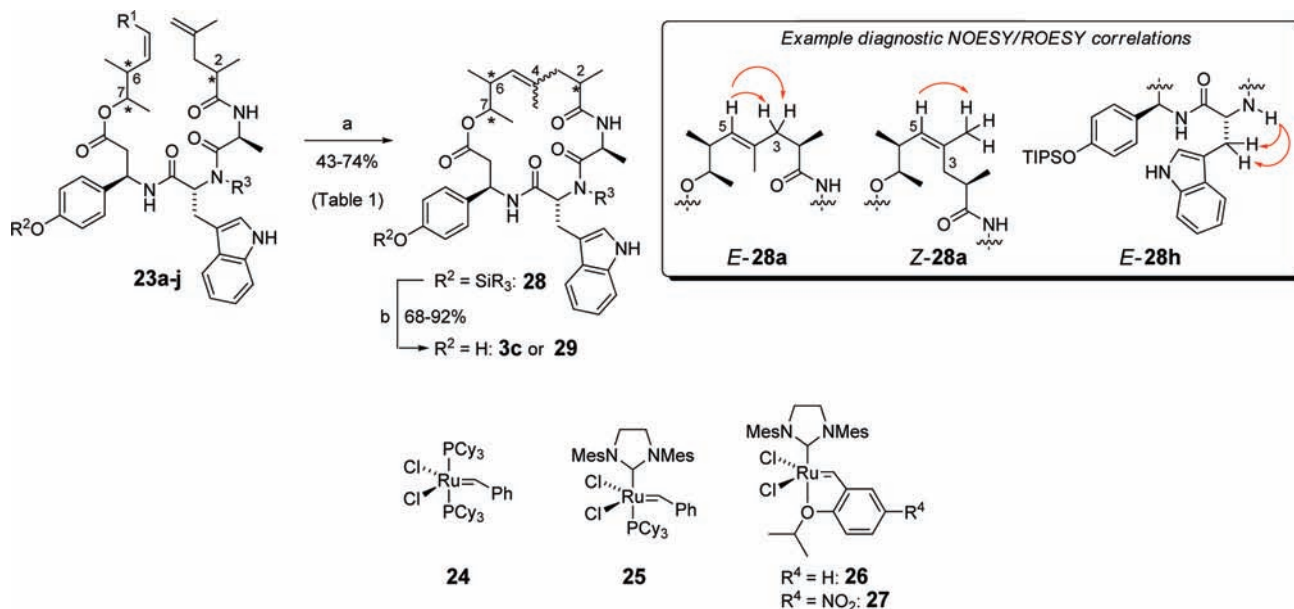
Macrocycle Formation by RCM: Chondramide C Analogues. The pivotal ring-closing metathesis (RCM) step was studied next. For the synthesis of macrocycle-embedded

(38) (a) White, K. N.; Konopelski, J. P. *Org. Lett.* **2005**, *7*, 4111. See also: (b) Ohfuné, Y.; Kurokawa, N.; Higuchi, N.; Saito, M.; Hashimoto, M.; Tanaka, T. *Chem. Lett.* **1984**, 441.
 (39) Hintermann, T.; Seebach, D. *Helv. Chim. Acta* **1998**, *81*, 2093.
 (40) Tannert, R.; Schürmann, M.; Preut, H.; Arndt, H.-D.; Waldmann, H. *Acta Crystallogr., Sect. E* **2007**, *63*, O4381.
 (41) Brown, H. C.; Bhat, K. S. *J. Am. Chem. Soc.* **1986**, *108*, 293.
 (42) Myers, A. G.; McKinstry, L. *J. Org. Chem.* **1996**, *61*, 2428.

(43) On cleavage of (OTBS)- or (OTIPS)- β -tyrosine-containing peptidic acids **11c–g** from the polymer support (Scheme 4), varying quantities of the phenolic OH unprotected form were additionally isolated (Supporting Information). Further investigations suggested that the peptide coupling conditions (carbodiimide in combination with amino acid and benzotriazole) were favoring undesired silyl deprotection. Fortunately, the desilylated peptides could be readily reprotected in solution using standard conditions (Supporting Information).
 (44) For a recent review see: But, T. Y. S.; Toy, P. H. *Chem. Asian J.* **2007**, *2*, 1340.

Scheme 4. Solid-Phase-Based Synthesis of Metathesis Precursors^a

^a Reagents and conditions: (a) **13a-c** (see Scheme 2 conditions a-d), 2-chlorotrityl chloride resin, (iPr)₂NEt, CH₂Cl₂, rt, 1 h; (b) DBU, piperidine, NMP (5 ×), rt; (c) **14a-c** (see Scheme 2, conditions e-k), DIC, HOBT, NMP or DMF, rt, 2-3 h; (d) Fmoc-α-Ala-OH, HATU, HOAt, (iPr)₂NEt, NMP, rt, 2-3 h; (e) *S*-**15** or *R*-**15** (see Scheme 2, conditions l, m), DIC or HATU, HOBT, (iPr)₂NEt, NMP, rt, 2-3 h; (f) HFIP/CH₂Cl₂ or AcOH/TFE/CH₂Cl₂ (1 × 20 min, 1 × 10 min); (g) **12a-f** for chondramide C analogues (*n* = 0) or **12h-i** for jasplakinolide analogues (*n* = 1) - see Scheme 3, EDC·HCl, (iPr)₂NEt, DMAP, CH₂Cl₂/DMF, rt, 14 h.

Scheme 5. Development of General Metathesis Conditions and Formation of Chondramide C (**3c**) and Analogues **28** and **29** (see Table 1)^a

^a Reagents and conditions: (a) conditions: see Table 1 conditions; (b) TBAF, THF, 30 min.

α-branched trisubstituted olefins by RCM, Grubbs' second-generation catalyst (Scheme 5, **25**)⁴⁵ has found frequent use, typically in refluxing CH₂Cl₂,⁴⁶ though the rates of conversion and the *E/Z*-selectivities were largely substrate dependent. For our purposes, treating diene **23a** with 10 mol % of **25** in degassed refluxing CH₂Cl₂ produced no conversion, even after further catalyst additions and extended heating (Table 1, entry 1). Disappointingly, more forcing conditions (Table 1, entry 2), and a switch to the Hoveyda-Grubbs second-generation or

Grela-type catalysts (Scheme 5, **26** and **27**),⁴⁷ did not improve the outcome (Table 1, entries 3 and 4).⁴⁸

To account for the steric hindrance of the C6-olefin methyl group, we next attempted ring closure using relay metathesis (RRCM).⁴⁹ Additionally, it was speculated that purging the reaction of ethylene with argon may improve catalyst reactivity.⁵⁰ We were pleased to find that treating precursor **23b** with 20 mol % of **25** in refluxing toluene with purging argon

(45) Scholl, M.; Ding, S.; Lee, C. W.; Grubbs, R. H. *Org. Lett.* **1999**, *1*, 953.

(46) (a) Alexander, M. D.; Fontaine, S. D.; La Claire, J. J.; DiPasquale, A. G.; Rheingold, A. L.; Burkhart, M. D. *Chem. Commun.* **2006**, 4602. (b) Smith, A. B., III; Mesaros, E. F.; Meyer, E. A. *J. Am. Chem. Soc.* **2006**, *128*, 5292. (c) Feyen, F.; Jantsch, A.; Altmann, K.-H. *Synlett* **2007**, 415. (d) Jin, J.; Chen, Y.; Li, Y.; Wu, J.; Dai, W.-M. *Org. Lett.* **2007**, *9*, 2585. For a recent review see: (e) Gradillas, A.; Pérez-Castells, J. *Angew. Chem.* **2006**, *118*, 8264. *Angew. Chem. Int. Ed.*, **2006**, *45*, 6086.

(47) (a) Garber, S. B.; Kingsbury, J. S.; Gray, B. L.; Hoveyda, A. H. *J. Am. Chem. Soc.* **2000**, *122*, 8168. (b) Grela, K.; Harutyunyan, S.; Michrowska, A. *Angew. Chem.* **2002**, *114*, 4210. *Angew. Chem., Int. Ed.* **2002**, *41*, 4038. (c) Review: Samojłowicz, C.; Bieniek, M.; Grela, K. *Chem. Rev.* **2009**, *109*, 3708.

(48) Conditions for generating sterically hindered olefins were tested as well: Rost, D.; Porta, M.; Gessler, S.; Blechert, S. *Tetrahedron Lett.* **2008**, *49*, 5968.

(49) For a recent review see: Wallace, D. *Angew. Chem.* **2005**, *117*, 1946. *Angew. Chem., Int. Ed.*, **2005**, *44*, 1912.

(50) Nosse, B.; Schall, A.; Jeong, W. B.; Reiser, O. *Adv. Synth. Catal.* **2005**, *347*, 1869.

Table 1. Synthesis of Chondramide C **3c**, Silyl-Protected Macrocycles **28**, and Chondramide C Analogues **29** (see Scheme 5)

entry	diene	R ¹	R ²	R ³	polyketide	cat.	mol %	solvent ^a	T/°C	t/h	E-isomer (yield/%)	Z-isomer (yield/%)
1	23a	H	TBS (–)	Me	2 <i>R</i> ,6 <i>S</i> ,7 <i>R</i>	25	10	CH ₂ Cl ₂ ^b	40	4	– ^d	– ^d
2	23a	H	TBS (–)	Me	2 <i>R</i> ,6 <i>S</i> ,7 <i>R</i>	25	25	PhMe ^b	85	4	– ^e	– ^e
3	23a	H	TBS (–)	Me	2 <i>R</i> ,6 <i>S</i> ,7 <i>R</i>	26	30	PhMe ^b	110	18	–	–
4	23a	H	TBS (–)	Me	2 <i>R</i> ,6 <i>S</i> ,7 <i>R</i>	27	25	PhMe ^b	110	4	– ^f	– ^f
5	23b	4-pentenyl	TBS (<i>E</i> - 28a / <i>Z</i> - 28a)	Me	2 <i>R</i> ,6 <i>S</i> ,7 <i>R</i>	25	20	PhMe ^c	110	3	<i>E</i> - 29a (14) ^{g,h,i}	<i>Z</i> - 29a (23) ^{g,h,i}
6	23c	4-pentenyl	TBS (<i>Z</i> - 28b)	Me	2 <i>R</i> ,6 <i>R</i> ,7 <i>S</i>	25	20	PhMe ^c	110	2	–	<i>Z</i> - 29b (33) ^{g,i}
7	23d	H	TBS (<i>E</i> - 28c)	Me	2 <i>R</i> ,6 <i>S</i> ,7 <i>S</i>	25	25	PhMe ^c	110	2	<i>E</i> - 29c (47) ⁱ	–
8	23e	H	TBS (–)	Me	2 <i>R</i> ,6 <i>R</i> ,7 <i>R</i>	25	25	PhMe ^c	110	2	–	–
9	23f	H	TIPS (<i>E</i> - 28d)	Me	2 <i>S</i> ,6 <i>R</i> ,7 <i>R</i>	25	25	PhMe ^c	110	2	3c (52) ⁱ	–
10	23g	H	TIPS (<i>E</i> - 28e / <i>Z</i> - 28e)	Me	2 <i>S</i> ,6 <i>S</i> ,7 <i>R</i>	25	25	PhMe ^c	110	2	<i>E</i> - 29e / <i>Z</i> - 29e (combined: 39) ^{i,j}	
11	23h	H	TIPS (<i>Z</i> - 28f)	Me	2 <i>S</i> ,6 <i>S</i> ,7 <i>S</i>	25	25	PhMe ^c	110	2	–	<i>Z</i> - 29f (44) ⁱ
12	23i	H	TIPS (<i>E</i> - 28g)	Me	2 <i>S</i> ,6 <i>R</i> ,7 <i>S</i>	25	25	PhMe ^c	110	2	<i>E</i> - 29g (62) ⁱ	–
13	23j	H	TIPS (<i>E</i> - 28h)	H	2 <i>S</i> ,6 <i>R</i> ,7 <i>R</i>	25	25	PhMe ^c	110	2	<i>E</i> - 29h (29) ⁱ	–

^a All solvents degassed prior to use. ^b 3 mM dilution. ^c 1 mM dilution and continuous argon purging. ^d No change after a further 20 mol % addition and 5 h. ^e No change after a further 30 mol % addition and overnight heating. ^f No change after a further 50 mol % addition and overnight heating. ^g Yield calculated over two steps including silyl-deprotection step (b). ^h 1:1.5 *E/Z* mixture after cyclization. ⁱ Yields determined after purification by column chromatography. ^j Inseparable 1:1.4 *E/Z* mixture; 1:1.1 after desilylation (R¹ = TIPS → H).

produced our first chondramide C analogues as a separable 1:1.5 mixture of *E/Z* isomers (*E*-**29a** and *Z*-**29a**) in yields of 14 and 23%, respectively, after deprotection of the silyl group (Table 1, entry 5). The same conditions were then successfully applied to diene **23c**, leading this time to a single isomer (*Z*-**29b**) in a promising 33% yield over two steps (Table 1, entry 6). Despite initial concerns raised by the non-reactivity of **23a**, we were fortunate to find that the newly developed metathesis conditions were generally applicable to the other dienes in the series **23d–j** (Table 1, entries 7–13) with the exception of **23e** (Table 1, entry 8). In each successful case, the geometric outcome of ring closure could conveniently be determined by NOESY or ROESY analysis (Scheme 5). The negligible turnover of dienes **23a** and **23e** nonetheless serves as an important reminder of the substrate dependency of the RCM methodology.⁵¹ Pleasingly, among the macrocycle products, the (2*S*,4*E*,6*R*,7*R*)-configured compound (Table 1, entry 9) was found to be identical to chondramide C (**3c**) by comparing compound characterization and cell screening data with those measured for material isolated from natural sources.^{19a}

On closer inspection of the metathesis results (Table 1), the *E/Z*-outcome appeared to be strongly influenced by the configuration of the polyketide, especially at the C2-position. First, while (2*R*,6*S*,7*R*)- and (2*S*,6*S*,7*R*)-configured dienes (**23b** and **23g**, respectively) both yielded 2:3 *E/Z* mixtures (Table 1, entries 5 and 10), the diene pair **23d** and **23h** instead produced *opposite* olefin geometries (Table 1, compare entries 7 and 11). A similar switch in selectivity was also observed in the case of dienes **23c** and **23i** (Table 1, compare entries 6 and 12). Finally, whereas **23f** reacted to form *E*-olefin **3c** (after silyl-deprotection

of *E*-**28d**), diene **23e** was *unreactive* (Table 1, compare entries 8 and 9). In each case, the stereochemistries of the diene precursors under comparison differ only by inversion at the C2-position. The observed selectivities are difficult to rationalize. However, we found that the *E/Z*-ratios did not evidently change during the course of the reaction, which suggests that double-bond formation takes place under kinetic control and that the geometric outcomes described in Table 1 result from distinct ruthenocyclobutane intermediate conformations.⁵² The *E/Z*-outcome is likely, therefore, to be independent of the metathesis strategy employed (consider **23c** and **23i**, RRCM vs RCM). In addition, minor structural changes to the phenolic silyl protecting group (Scheme 5, R²) are not believed to influence *E/Z*-product ratios (consider **23e** and **23f**, for example), although the effect of remote functional groups on ring formation can be strong,⁵³ while proximal groups such as α -olefinic substituents are known to significantly influence the reactivity and selectivity of RCM processes.⁵⁴ Indeed, kinetically controlled RCM of densely functionalized dienes in the context of natural product synthesis has been previously reported.⁵⁵

D-Amino acids are known to induce type-II' β -turns,⁵⁶ and *N*-methylated amino acids lower the energy difference between the *cis*- and *trans*-conformation of peptide bonds, leading to

(51) Diene **23f** was treated once with catalyst **25** in refluxing CH₂Cl₂ without reaction (data not shown) to indicate that the non-reactivity of diene **23a** is indeed representative of all diene substrates.

(52) Grubbs, R. H., Ed. *Handbook of Metathesis*; Wiley-VCH: Weinheim, 2003; Vols. 1–3.

(53) Fürstner, A.; Thiel, O. R.; Blanda, G. *Org. Lett.* **2000**, *2*, 3731.

(54) Ramírez-Fernández, J.; Collado, I. G.; Hernández-Galán, R. *Synlett* **2008**, 339.

(55) For a related example see: (a) Castoldi, D.; Caggiano, L.; Panigada, L.; Sharon, O.; Costa, A. M.; Gennari, C. *Angew. Chem.* **2005**, *117*, 594. *Angew. Chem., Int. Ed.* **2005**, *44*, 588. (b) Castoldi, D.; Caggiano, L.; Panigada, L.; Sharon, O.; Costa, A. M.; Gennari, C. *Chem.–Eur. J.* **2006**, *12*, 51.

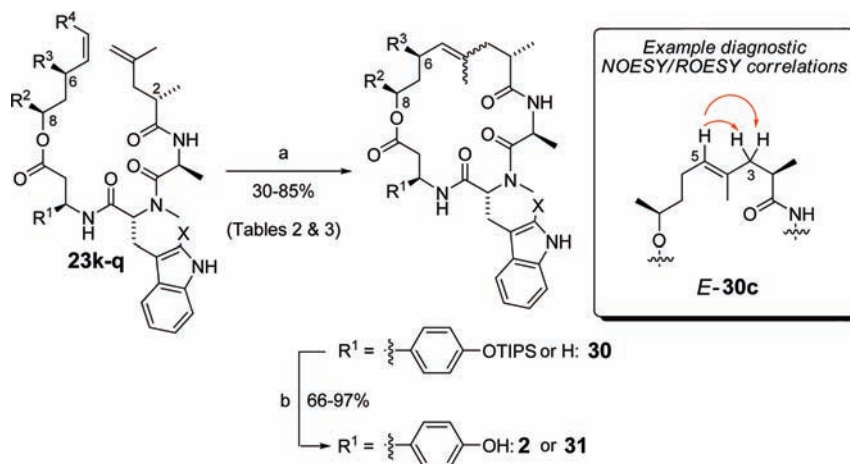
(56) Heller, M.; Sukopp, M.; Tsomaia, N.; John, M.; Mierke, D. F.; Reif, B.; Kessler, H. *J. Am. Chem. Soc.* **2006**, *128*, 13806.

Table 2. Synthesis of Jasplakinolide/Jaspamide **2**, Silyl-Protected Macrocycles **30** and Jasplakinolide Analogues **31** (see Scheme 6)

entry	diene	R ¹	R ²	R ³	R ⁴	X	E-isomer (yield/%)	Z-isomer (yield/%)
1	23k	4-(OTIPS)-C ₆ H ₄ (<i>E</i> - 30a / <i>Z</i> - 30a)	Me	Me	H	Br	2 (10) ^{a,b}	<i>Z</i> - 2 (18) ^{a,b}
2	23l	4-(OTIPS)-C ₆ H ₄ (<i>E</i> - 30b / <i>Z</i> - 30b)	Me	Me	H	H	<i>E</i> - 31b (14) ^{a,c}	<i>Z</i> - 31b (18) ^{a,c}
3	23m	4-(OTIPS)-C ₆ H ₄ (<i>E</i> - 30b / <i>Z</i> - 30b)	Me	Me	4-pentenyl	H	<i>E</i> - 31b (27) ^{a,c}	<i>Z</i> - 31b (24) ^{a,c}
4	23n	4-(OTIPS)-C ₆ H ₄ (<i>E</i> - 30c)	Me	H	H	H	<i>E</i> - 31c (58) ^{a,c,d}	–
5	23o	4-(OTIPS)-C ₆ H ₄ (<i>E</i> - 30d)	H	H	H	H	<i>E</i> - 31d (68) ^{a,c,e}	–
6	23p	H	Me	H	H	H	<i>E</i> - 31e (85) ^{c,d}	–
7	23q	H	H	H	H	H	<i>E</i> - 31f (76) ^{c,e}	–

^a Calculated over two steps. ^b Yield determined after column chromatography and preparative HPLC purification. ^c Yield determined after column chromatography purification. ^d 5 mol %, then heating for a further 5 min (10 min in total). ^e 6 × 5 mol % (every 5 min), then heating for a further 30 min.

Scheme 6. Formation of Jasplakinolide/Jaspamide **2** and Analogues **30** and **31** by Ring-Closing Metathesis (see Tables 2 and 3)^a



^a Reagents and conditions: (a) **25** (25–30 mol %, single-portion), PhMe (degassed, 1 mM), reflux, argon purging, 2 h; (b) TBAF, THF, 30 min see Tables 2 and 3.

the loss of a potentially important hydrogen donor in the backbone of peptide-based structures.⁵⁷ In this context, the *N*-Me-Trp- β Tyr- sequence of **2** has been surmised to adopt a type-II β -turn conformation,³² a proposal that has led a number of research groups to prepare macrocyclic analogues bearing this sequence alone in the peptide region.^{32,58} In order to study the influence of *N*-methylation on the macrocycle conformation, and quantify its impact on cytotoxicity, we synthesized *E*-**29h**, norchondramide C (Table 1, entry 13) by replacing D-abrine with D-tryptophan in the course of the synthesis (Schemes 4 and 5). Compared with the formation of **3c** (Table 1, entry 9), the lack of *N*-methylation in diene **23j** (Table 1, entry 13) did not evidently alter the outcome of the metathesis reaction (predominantly *E*). The same preference for the *trans*-amide bond rotamer was observed according to NOESY experiments (Scheme 5), although the reaction's yield was somewhat lower.

Macrocycle Formation by RCM: Jasplakinolide Analogues. The synthesis of jasplakinolide/jaspamide (**2**) and the desbromo-analogue *E*-**31b** by RCM proved to be equally challenging (Table 2). Nonetheless, using the previously established metathesis conditions, cyclization was successful, in each case yielding approximately 1:1 *E/Z* mixtures, which were separable by chromatography (Table 2, entries 1 and 2). The relay RCM approach was also successful (Table 2, entry 3) and slightly higher yielding, but did not produce any significant change in *E/Z*-selectivity. Indeed, HPLC analysis of the crude RCM and RRCM mixtures revealed a nearly identical formation of *E/Z* isomers to suggest that the macrocycle-forming cycloaddition–cycloreversion steps are rate-determining. In stark contrast, analogues lacking a methyl group at the C6 position of the polyketide (Scheme 6, R³ = H) were significantly more straightforward to prepare. Under similar conditions, dienes **23n–q** were fast to react and high yielding and led almost exclusively to the *E*-isomer (Table 2, entries 4–7). A more rigorous control of the rate of conversion of substrates **23n** and **23p** showed the transformation to be complete within 10 min using only 5 mol % of catalyst.

- (57) (a) Chatterjee, J.; Mierke, D.; Kessler, H. *J. Am. Chem. Soc.* **2006**, *128*, 15164. (b) Dechantsreiter, M. A.; Planker, E.; Mathä, B.; Lohof, E.; Hölzemann, G.; Jonczyk, A.; Goodman, S. L.; Kessler, H. *J. Med. Chem.* **1999**, *42*, 3033.
- (58) Celanire, S.; Descamps-Francois, C.; Lesur, B.; Guillaumet, G.; Joseph, B. *Lett. Org. Chem.* **2005**, *2*, 528.

Table 3. Optimization of Metathesis Conditions for Non- α -branched Dienes **23n–q** (see Table 2 and Scheme 6)

entry	diene	cat.	mol % ^a	T/°C	t/h	conv./%	prod (yield/%) ^b
1	23n	25	5	23	24	30 ^c	<i>E</i> - 30c (n.d.)
2	23n	25	10	40	3	89 ^d	<i>E</i> - 30c (65)
3	23n	24	10	40	24	<5 ^c	n.d.
4	23n	26	10	40	24	65 ^c	<i>E</i> - 30c (n.d.)
5	23o	25	5	40	15	57 ^d	<i>E</i> - 30d (30)
6	23p	25	5	40	3	91 ^d	<i>E</i> - 30e (75)
7	23q	25	5	40	15	75 ^d	<i>E</i> - 30c (59)

^a Single portion addition. Reaction run in degassed CH₂Cl₂ at 1 mM substrate concentration. ^b Preparative yield, n.d. = not determined. ^c By integration of crude HPLC trace. ^d By integration of crude ¹H NMR signals.

This significant increase in metathesis reactivity for substrates lacking the methyl group at the C6 position of the polyketide allowed us to realize milder conditions. We were gratified to find, therefore, that treating **23n** with 5 mol % of **25** in dry CH₂Cl₂ at room temperature resulted in a 30% conversion to *E*-**30c** within 24 h (Table 3, entry 1). This promising result could be further optimized by using 10 mol % of catalyst and heating at 40 °C for 3 h, leading to an 89% conversion and isolated yield of 65% (Table 3, entry 2). When the results for **30b** and **31b** (Table 2, entries 2 and 3) and **30c** (Table 3, entry 2) are compared, it becomes apparent how the C6-methyl group influences the reactivity and *E/Z*-selectivity of ring-closure. Catalyst **24**⁵⁹ failed to catalyze ring closure (Table 3, entry 3), while catalyst **26** managed a useful conversion (Table 3, entry 4) to add further scope to this reaction. Indeed, for our purposes, these conditions were found to be quite general for analogous substrates (Table 3, entries 5–7) to provide further complex examples of macrocycle-embedded trisubstituted olefin formation using RCM under mild reaction conditions.⁴⁶

In summary, for the formation of macrocycle-embedded α -methyl olefins, forcing conditions were required: 25–30 mol % of catalyst **25** in dry, degassed toluene (1 mM) heating under reflux for 2 h with continuous argon purging. In the case of

non- α -methyl-substituted olefins, milder conditions proved effective: 5–10 mol % catalyst **25** in dry CH₂Cl₂ (1 mM) heating at 40 °C for 3–15 h.

Biological Evaluation. Chondramide C Analogues. Recently, a study on a series of novel natural jasplakinolide/jaspamide analogues reported compound isolation, rigorous structure elucidation by NMR analysis, and the determination of compound cytotoxicity toward MCF-7 and HT-29 cancer cells.⁶⁰ To allow comparison, we tested our synthetic analogues against the same cell lines (Table 4). In general the (2*R*)-configured analogues were significantly less potent than their corresponding (2*S*)-isomers. The two (2*R,4Z*)-isomers showed some remaining activity (Table 4, entries 6 and 7), while the (2*R,4E*)-configured analogues were completely inactive (Table 4, entries 5 and 8). By contrast, the (2*S*)-isomers (Table 4, entries 9–11) were only 10–100-fold less potent than synthetic **3c** (Table 4, entry 2), which itself was found to be equipotent with the natural product (Table 4, entry 1) as final confirmation to a successful total synthesis.^{19a} The fact that *Z*-**29f** was also active within the same range is an indication that changes in olefin geometry modulate but do not extinguish biological activity. During work toward their own total synthesis of **3c**, Kalesse and co-workers observed similar levels of cytotoxicity for a number of (2*S,4E*)-configured isomers against different cancer cell lineages (Figure 3, *E*-**29e**, *E*-**29f**, and *E*-**29g**), including one that was equally potent as **3c**.^{19b} Indeed, the (2*S,4E*)-stereochemical arrangement is a structural hallmark of jaspamide/jasplakinolide, geodiamolide, and seragamide families (Figure 1). Furthermore, compared with **2**, synthetic (2*R*)-**2** was reported to display different insect anti-feedant properties⁶¹ while the natural analogue jaspamide **J** (Figure 3, **32a**)⁶⁰ was 100-fold less cytotoxic. Methylation of the tryptophan α -amino group could also be considered essential for optimal potency on the basis of our result for norchondramide **C**, *E*-**29h** (Table 4, entry 12), where an approximate 10-fold loss in activity was observed. In support of this, the natural analogue jaspamide **M** (Figure 3, **32b**), also lacking the *N*-methylation, was found to be one-order-of magnitude less

Table 4. Cytotoxicity Data for Chondramide C **3c** and Analogues **28** and **29**

entry	no.	R ²	R ³	polyketide	MCF-7 IC ₅₀ /μM (±)	HT-29 IC ₅₀ /μM (±)
1	3c ^a	H	Me	2 <i>S,4E,6R,7R</i>	0.023 (0.002)	0.021 (0.001)
2	3c ^b	H	Me	2 <i>S,4E,6R,7R</i>	0.083 (0.004)	0.031 (0.001)
3	<i>Z</i> - 28a	TBS	Me	2 <i>R,4Z,6S,7R</i>	10.2 (0.62)	>15.0 (–)
4	<i>E</i> - 28d	TIPS	Me	2 <i>S,4E,6R,7R</i>	2.33 (0.25)	2.64 (0.52)
5	<i>E</i> - 29a	H	Me	2 <i>R,4E,6S,7R</i>	>15.0 (–)	>15.0 (–)
6	<i>Z</i> - 29a	H	Me	2 <i>R,4Z,6S,7R</i>	3.17 (0.49)	3.71 (0.82)
7	<i>Z</i> - 29b	H	Me	2 <i>R,4Z,6R,7S</i>	6.85 (1.10)	6.19 (1.17)
8	<i>E</i> - 29c	H	Me	2 <i>R,4E,6S,7S</i>	>15.0 (–)	>15.0 (–)
9	<i>E</i> - 29e / <i>Z</i> - 29e ^c	H	Me	2 <i>S,6S,7R</i>	0.34 (0.089)	0.31 (0.028)
10	<i>Z</i> - 29f	H	Me	2 <i>S,4Z,6S,7S</i>	0.21 (0.016)	0.28 (0.012)
11	<i>E</i> - 29g	H	Me	2 <i>S,4E,6R,7S</i>	0.39 (0.033)	0.70 (0.050)
12	<i>E</i> - 29h	H	H	2 <i>S,4E,6R,7R</i>	0.22 (0.017)	0.19 (0.010)

^a Natural source. ^b Synthetic material. ^c Inseparable 1:1.1 *E/Z* mixture.

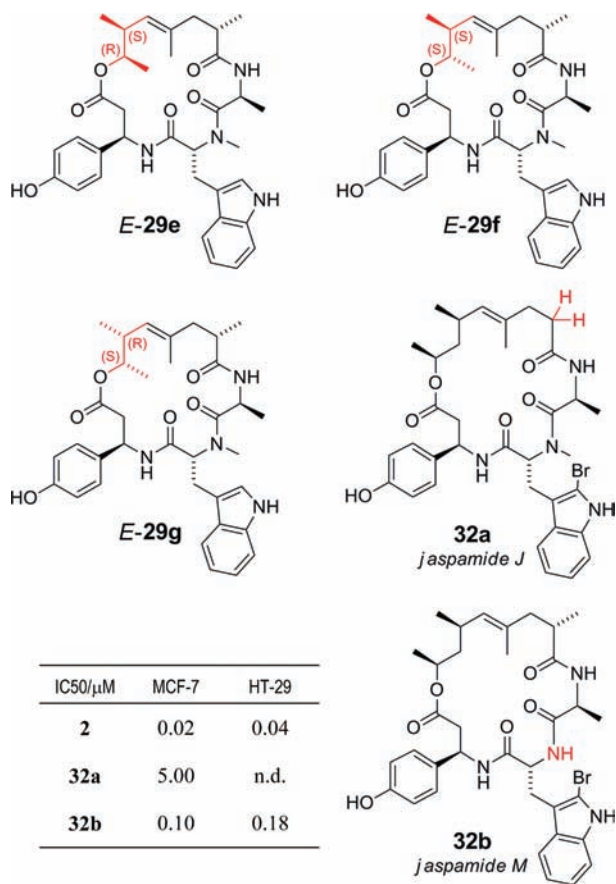


Figure 3. Previously reported cytotoxicity data for synthetic and natural analogues of **2**⁶⁰ and chondramide C (**3c**).^{19b}

potent than **2**.⁶⁰ Finally, the relative inactivity of OTBS- and OTIPS-protected analogues **Z-28a** and **E-28d** (Table 4, entries 3 and 4) strongly suggest that substituting the phenolic OH with sterically bulky groups is not well tolerated. In summary, these results indicate the extent by which the polyketide configuration dictates the biological activity of **3c**. The stereochemical arrangement at C2 appears to be particularly sensitive to variation, while the configuration at C6 and C7, *N*-methylation, and even the olefin geometry adopt a more fine-tuning role, leading in some cases to equally potent conformational manifolds.^{19b}

Jasplakinolide Analogues. Jasplakinolide (**2**) and five simplified analogues were screened for cytotoxicity toward MCF-7 and HT-29 cancer cell lines as well (Table 5). The desbromo

analogue, **E-31b** (Table 5, entry 2),⁶² recently isolated from nature as jaspamide Q,⁶³ was essentially equipotent with **2** to suggest that the indole-based bromine atom is not required for potent activity. This result might be considered general, as halogenated and non-halogenated members of the chondramide family share the same potent cytotoxic properties (A–D, Figure 4, **3a–d**)^{18,20}—despite the recurrence of aromatic halogenation in nearly all known natural jaspamide,⁶⁰ geodiamolide,^{10c,21,22} seragamide²³ family members as well as dolicolide.^{24,25} In this context, an interesting fine-tuning of compound potency and selectivity has been demonstrated through variation of the halogen group.^{22,24c}

Two natural analogues of jaspamide lacking methyl substituents in the polyketide region of the molecule (Figure 4, **32c** and **32d**) were recently shown to be significantly inactive toward MCF-7 cells ($IC_{50} > 30 \mu M$).⁶⁰ This strong drop in activity was attributed to a loss in actin-binding affinity and related to an increase in ring flexibility through the simultaneous loss of 1,3-allylic and/or *syn*-pentane interactions.^{29a} On the contrary, however, we were surprised to find the newly synthesized analogue **E-31c** to be only 2-fold less potent and **E-31d** no greater than 10-fold less active (entries 3 and 4, Table 5). Indeed, early NMR and molecular mechanics studies into the solution-phase conformation of **2** identified conformational promiscuity in the C6–C8 region of the polyketide.⁶¹ This suggests that configurational or structural changes in this region of the molecule do not dramatically interfere with F-actin binding. On the other hand, β -alanine analogues **E-31e** and **E-31f** suffered a dramatic drop in activity (Table 5, entries 5 and 6), possibly due to the loss of stabilizing hydrophobic and/or hydrogen-bonding interactions at the putative actin-binding site.^{19a} Alternatively, the loss of one stereocenter leading to greater macrocycle flexibility and the breakdown of a potential type-II β -turn may be the determining factor.³²

To correlate cytotoxicity with the F-actin polymerizing properties of these compounds, immunofluorescence cell imaging was then performed by treating BSC-1 cells with **2**, **3c**, and synthetic analogues **E-31c** and **E-31e** (Figure 5). In DMSO (Figure 5A), a well-differentiated actin cytoskeleton including stress fibers can be clearly observed that becomes disorganized in the presence of the compounds (Figure 5B–E). At the half maximal toxic concentration (IC_{50}), a similar phenotype effect is observed—the stress fibers completely disappear, and actin lump formation occurs, preferentially in the perinuclear region. In summary, these results appear to indicate that, while the phenolic group is indispensable for activity, **2** can be structurally simplified in the case of **E-31b**, **E-31c**, and **E-31d** without significant loss in cytotoxicity and actin specificity.

Molecular Modeling Studies. From the biological data it was clear that all analogues show the phalloidin phenotype, which is caused by stabilizing the F-actin fibers through binding at the contact point of three independent monomers (Figure 6). To better explain some of the observed SAR trends, we

(59) (a) Schwab, P.; France, M. B.; Ziller, J. W.; Grubbs, R. H. *Angew. Chem.* **1995**, *107*, 2179. *Angew. Chem., Int. Ed.* **1995**, *34*, 2039. (b) Schwab, P.; Grubbs, R. H.; Ziller, J. W. *J. Am. Chem. Soc.* **1996**, *118*, 100. (c) Belderrain, T. R.; Grubbs, R. H. *Organometallics* **1997**, *16*, 4001.

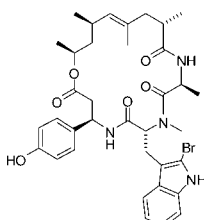
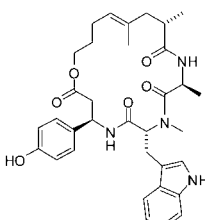
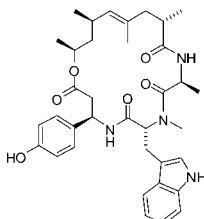
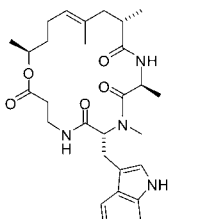
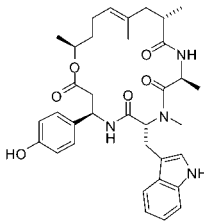
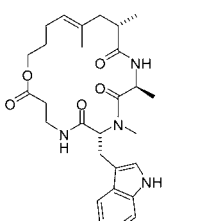
(60) (a) Gala, F.; D'Auria, M. V.; De Marino, S.; Zollo, F.; Smith, C. D.; Copper, J. E.; Zampella, A. *Tetrahedron* **2007**, *63*, 5212. (b) Gala, F.; D'Auria, M. V.; De Marino, S.; Sepe, V.; Zollo, F.; Smith, C. D.; Copper, J. E.; Zampella, A. *Tetrahedron* **2008**, *64*, 7127. (c) Gala, F.; D'Auria, M. V.; De Marino, S.; Sepe, V.; Zollo, F.; Smith, C. D.; Keller, S. N.; Zampella, A. *Tetrahedron* **2009**, *65*, 51.

(61) Inman, W.; Crews, P. *J. Am. Chem. Soc.* **1989**, *111*, 2822.

(62) Ebada, S. S.; Wray, V.; de Voogd, N. J.; Deng, Z.; Lin, W.; Proksch, P. *Mar. Drugs* **2009**, *7*, 435.

(63) Tannert, R.; Hu, T.-S.; Arndt, H.-D.; Waldmann, H. *Chem. Commun.* **2009**, 1493.

Table 5. Cytotoxicity Data for Jasplakinolide/Jasplamide 2 and Analogues 31

entry	no.	structure	MCF-7 IC ₅₀ /μM (±)	HT-29 IC ₅₀ /μM (±)	entry	no.	structure	MCF-7 IC ₅₀ /μM (±)	HT-29 IC ₅₀ /μM (±)
1	2		0.025 (0.004)	0.021 (0.004)	4	<i>E</i> -31d		0.085 (0.010)	0.168 (0.039)
2	<i>E</i> -31b		0.023 (0.009)	0.011 (0.004)	5	<i>E</i> -31e		>15.0 (-)	>15.0 (-)
3	<i>E</i> -31c		0.040 (0.003)	0.026 (0.001)	6	<i>E</i> -31f		>15.0 (-)	>15.0 (-)

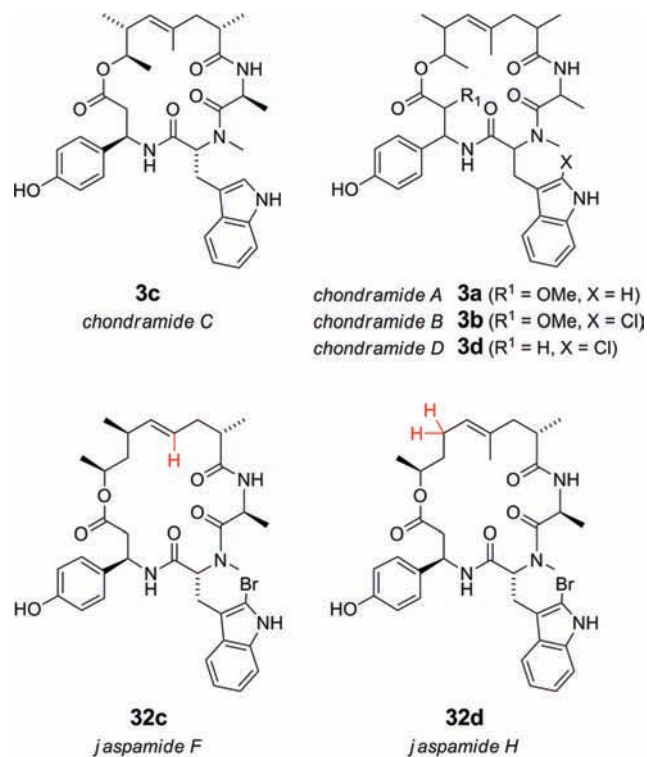
performed an overlay of a higher-resolution structure of F-actin in the ‘unbound’ state reported recently²⁷ with our previously published binding model of **3c** (the ‘bound’ state) derived from phalloidin-bound F-actin (Figure 6).^{19a} The overall structures of the actin polymers appear quite similar (Figure 6A), but local differences exist that could possibly result from ligand binding. In particular, the Tyr-198 and Phe-200 residues present on G-actin unit X (Figure 6) would appear to ‘move’ to enable favorable interactions with the hydrophobic indole moiety of the macrocycle in this flexible loop region.⁶⁴ However, more detailed conclusions must await higher-resolution structural data.

To our delight, our previously proposed binding mode for **3c** is supported by the bioactivity trends observed (Figure 6, B and C). The α -substituted carboxyl region (C1–C3) of the macrocycle polyketide is located close to the protein surface (Figure 6, B and C, red), whereas the C4–C5 olefin is apparently afforded more space. It could be argued, therefore, that the polyketide is of equal importance to the peptide for molecular recognition at the binding cleft and not just for tethering the peptide in the biologically active conformation. For example, the inactivity (>15 μ M) of chondramide C analogues *E*-29a and *E*-29c (Table 4, entries 5 and 8, respectively), both bearing the unnatural (*2R*)-configuration in combination with the natural *E*-olefin geometry, might be better explained by unfavorable steric interactions rather than by the population of undesirable peptide conformations that stem from this single modification. We even found moderately active examples (Table 4, entries 6 and 7) where the unnatural *Z*-olefin geometry apparently permits a ‘better fit’ of the (*2R*)-configured polyketide. Furthermore, the activity for analogues carrying the natural (*2S*)-configuration

and the unnatural *Z*-olefin geometry (Table 4, entries 9 and 10) was only attenuated by one-order-of-magnitude, hinting at a greater tolerance of structural change at this position (Figure 6, B and C, orange). Crucially, the dimethylhydroxyl portion of the polyketide (C6–C7) can be seen extending out into the cleft and is the region where structural change is tolerated most (Figure 6, B and C, green). For analogues of **3c**, changes in stereochemistry in this region will force the macrocycle into different conformational manifolds that lead to unfavorable binding. While this may be the case, we (Table 4, entries 9–11) and others (Figure 3)^{19b} have found such analogues to be still quite active—in general, only 10-fold less potent than **3c**, and in one case, resulting in an equipotent compound.^{19b} For analogues of **2**, the potency of *E*-31c and *E*-31d (Table 4, entries 3 and 4) is supported well by this binding model. The slight loss in activity observed in the case of *E*-31d might be explained by an increase in macrocycle flexibility. This model also offers an explanation for the fact that differences in ring size effective in this region of the polyketide [for example between jasplakinolide (**2**, 19-membered ring) and chondramide C (**3c**, 18-membered ring)] do not strongly impact on activity.

Activity trends can also be rationalized in the peptide region of the macrocycle. For example, the phenolic group of the β -tyrosine residue of **3c** is found protruding into a spacious cavity, though not fully exposed, with the phenolic hydroxyl group in close proximity (1.9–2.8 Å) to Asp-286 on G-actin monomer Y, suggesting a favorable stabilizing hydrogen-bonding interaction (see Supporting Information). In view of this, it is of no surprise that substituting the phenolic OH of **3c** with a bulky silyl-protecting group significantly impairs activity (Table 4, compare entries 1 and 2 with 4). The weak activity (IC₅₀ > 15 μ M) of jasplakinolide analogues *E*-31e and *E*-31f

(64) All pictures were rendered and analyzed using PyMol, V0.99; DeLano Scientific Ltd.: Palo Alto, CA.



IC ₅₀ /μM	U-937	A-431	A-498	A-549	SK-OV-3
3a	0.012	0.015	0.085	0.033	0.020
3b	0.012	0.010	0.015	0.015	0.006
3c	0.006	0.005	0.055	0.018	0.008
3d	0.003	0.005	0.015	0.014	0.005

IC ₅₀ /μM	MCF-7	HT-29
2	0.02	0.04
32c	30.0	n.d.
32d	30.0	n.d.

Figure 4. Literature data for chondramides A–D (**3a–d**)^{18,20} and jaspamides F and H (**32c,d**).⁶⁰

(Table 5, entries 5 and 6) might then be rationalized by a loss of the putative hydrogen bond to Asp-286, fewer hydrophobic interactions and an increase in macrocycle flexibility that all systematically weaken binding (see Supporting Information).

Conclusion

Using a novel approach, a focused collection of structurally and stereochemically diverse cyclodepsipeptides has been prepared including the total synthesis of jaspalakinolide/jaspamide (**2**) and chondramide C (**3c**). The synthesis is highlighted by an efficient solid phase-based preparation of the linear peptide-based chain followed by a rewarding ruthenium-catalyzed ring-closing metathesis of the macrocycle. In this case, metathesis reactivity and *E/Z*-selectivity was shown to strongly depend on the stereochemical configuration of the polyketide region of the molecule, especially the influence of an olefinic α -methyl substituent. The activity of synthetic analogues lacking indole

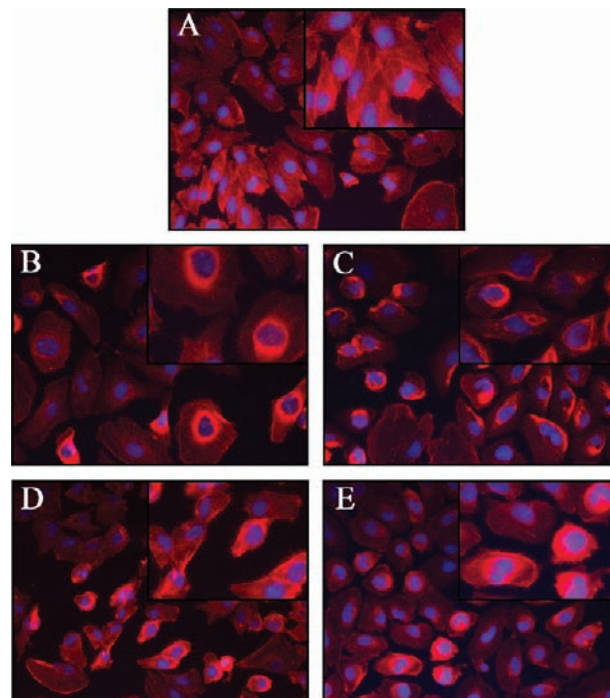


Figure 5. Representative immunofluorescence microscopy images of BSC-1 cells after 24 h of co-culture with different cyclodepsipeptides close to their respective IC₅₀ concentrations (magnification 20 \times , insert 40 \times). Actin is stained red (FITC-phalloidin, Invitrogen) and DNA blue (DAPI, Sigma-Aldrich). (A) DMSO; (B) **2** (25 nM); (C) **3c** (100 nM); (D) *E*-**31c** (50 nM); (E) *E*-**31e** (15 μ M).

bromination or *N*-methylation was shown to correlate well with relevant data for natural analogues. We have identified the key role played by the phenolic ring of the β -tyrosine moiety for compound activity. By comparing analogues of chondramide C (**3c**), we indicate how changes in polyketide stereochemistry determine cytotoxicity and rationalize structure–function trends in terms of a unified binding mode. In this way, we can explain the promiscuity of the C6–C7 region with respect to stereochemical variation. In support of this argument, we identified analogues of **2** lacking methyl substituents in this region of the polyketide that retained potent cytotoxicity and the characteristic actin-interfering phenotype profile. On the synthetic plane, the reduced complexity of potent analogues *E*-**31c** and *E*-**31d** has greatly facilitated the preparation by improving the *E/Z*-selectivity, yield and reaction conditions (40 $^{\circ}\text{C}$, 5 mol % catalyst) of the pivotal RCM-mediated macrocycle-forming step. Furthermore, the total number of discrete steps from commercial starting materials has been reduced from 32 to 22 (comparing our synthesis of **2** with that of *E*-**31c** and *E*-**31d**). The longest linear sequence has been reduced to 15 steps when counting all the trivial operations on solid phase. Overall, the synthetic status reached is of considerable effectiveness and is expected to facilitate future syntheses of more extensive macrocycle libraries and of structurally simplified actin-modulator tool compounds.

Experimental Procedures

Example Steglich Esterification Conditions: L-Pea-Ala-D-MeTrp- β Tyr(OTIPS)-O-(2*S*)-Hex (23n). The peptide acid **11d** (100 mg, 140 μ mol - see Supporting Information for details of synthesis) was dissolved under an argon atmosphere in CH_2Cl_2 (2.5 mL) and DMF (0.25 mL). At 23 $^{\circ}\text{C}$, (*S*)-5-Hexen-2-ol **12k** (42 mg, 0.42 mmol, 4.0 equiv), DMAP (34 mg, 0.28 mmol, 2.0 equiv), DIPEA

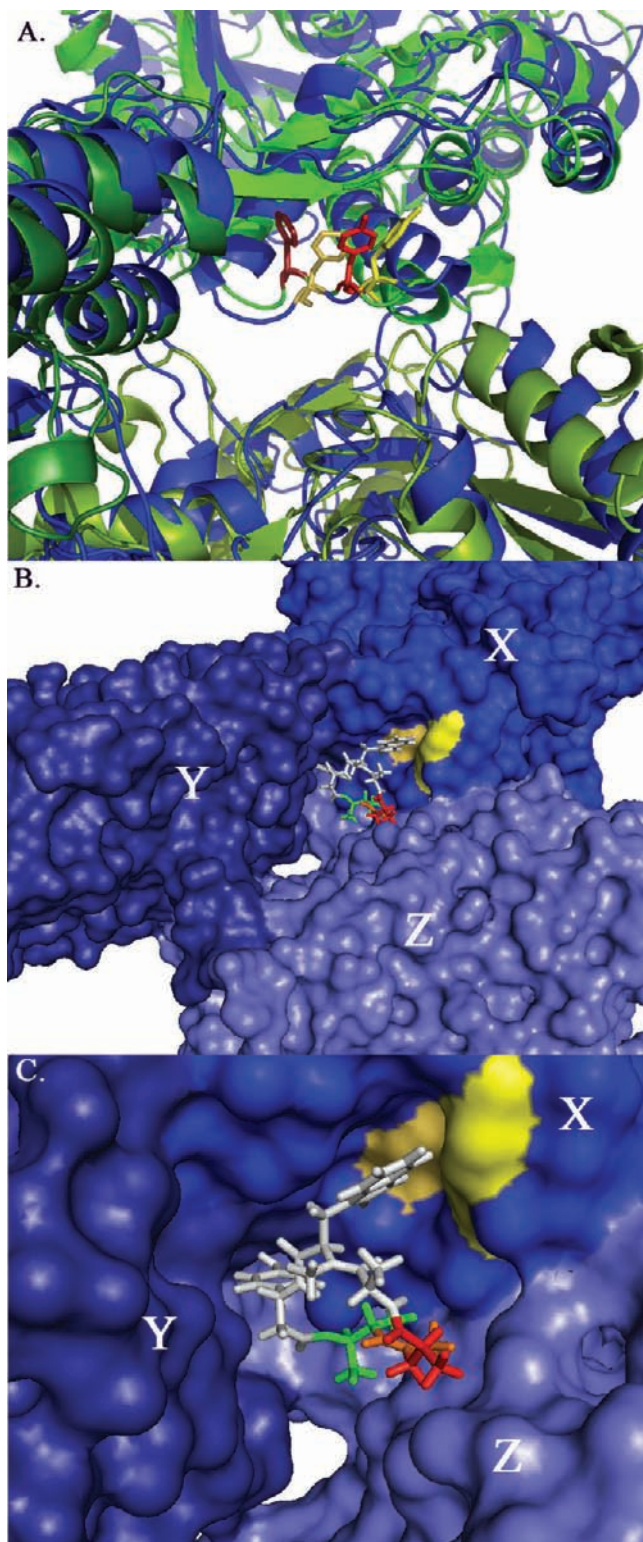


Figure 6. (A) Graphical overlay of the ‘bound’ (blue, lower resolution) and ‘unbound’ (green, higher resolution) structures of F-actin and the phalloidin binding cleft. In the unbound state, the three actin subunits are assigned three different shades of green. Amino acid residues Tyr-198 and Phe-200 are colored differently in the bound (yellow and pale yellow) and unbound (red and dark red) states. (B) Expanded space-fill model of the bound F-actin structure with bound **3c**.^{19a} The three independent actin subunits (X, Y, and Z) are labeled in three different shades of blue. (C) Close-up of the binding cleft: Regions where structural changes lead to a complete loss of activity are labeled red; regions that weaken but do not extinguish bioactivity are colored orange; changes that are tolerated are shaded green. The Tyr-198 and Phe-200 residues of the actin monomer unit X are highlighted yellow and pale yellow.⁶⁴

(49 μL , 0.28 mmol, 2.0 equiv), and finally EDC $\cdot\text{HCl}$ (53 mg, 0.28 mmol, 2.0 equiv) were added sequentially to the colorless solution. The mixture was stirred for 19 h, diluted with AcOEt (20 mL), and washed with a saturated aqueous solution of NH_4Cl (2×10 mL). The aqueous layer was extracted with AcOEt (20 mL), and the combined organic extracts were washed with brine (20 mL), dried (Na_2SO_4), filtered, and concentrated. Column chromatography (AcOEt/cyclohexane) of the crude material yielded the desired peptide diene **23n** (95 mg, 120 μmol , 85%) as a clear colorless wax.

$R_f = 0.25$ (AcOEt/cyclohexane 1:1); LC: $t_R = 12.04$ min (Method A - see Supporting Information); $[\alpha]_D = +20.4$ ($c = 1.0$ in CHCl_3); ^1H NMR (400 MHz, CDCl_3): mixture of rotamers (ratio $> 7:1$), major rotamer: δ 8.09 (s, 1H; Trp2-NH), 7.59 (d, $^3J = 7.8$ Hz, 1H; Trp4-H), 7.32 (d, $^3J = 8.0$ Hz, 1H; Trp7-H), 7.19–7.09 (m, 3H; Trp6-H, Trp5-H, $\beta\text{Tyr}\beta\text{-NH}$), 7.09 (d, $^3J = 8.5$ Hz, 2H; $\beta\text{Tyr}2\text{-H}$, $\beta\text{Tyr}6\text{-H}$), 6.94 (s, 1H; Trp2-H), 6.76 (d, $^3J = 8.5$ Hz, 2H; $\beta\text{Tyr}3\text{-H}$, $\beta\text{Tyr}5\text{-H}$), 6.34 (d, $^3J = 6.1$ Hz, 1H; Ala $\alpha\text{-NH}$), 5.71 (ddt, $^3J = 16.9/10.2/6.6$ Hz, 1H; Hex5-H), 5.56 (dd, $^3J = 10.3/5.9$ Hz, 1H; Trp $\alpha\text{-H}$), 5.36 (dd, $^3J = 14.8/7.1$ Hz, 1H; $\beta\text{Tyr}\beta\text{-H}$), 4.94 (dd, $^3J = 17.2$ Hz, $^2J = 1.6$ Hz, 1H; Hex6- H_{trans}), 4.92 (d, $^3J = 10.1$ Hz, 1H; Hex6- H_{cis}), 4.86–4.77 (m, 1H; Hex2-H), 4.77 (s, 1H; Pea5- H_a), 4.70 (s, 1H; Pea5- H_b), 4.61 (dq, $^3J = 6.8/6.8$ Hz, 1H; Ala $\alpha\text{-H}$), 3.46 (dd, $^3J = 5.9$ Hz, $^2J = 15.7$ Hz, 1H; Trp $\beta\text{-H}_a$), 3.21 (dd, $^3J = 10.5$ Hz, $^2J = 15.7$ Hz, 1H; Trp $\beta\text{-H}_b$), 2.94 (s, 3H; Trp-NCH $_3$), 2.90 (dd, $^3J = 7.4$ Hz, $^2J = 15.2$ Hz, 1H; $\beta\text{Tyr}\alpha\text{-H}_a$), 2.75 (dd, $^3J = 6.2$ Hz, $^2J = 15.2$ Hz, 1H; $\beta\text{Tyr}\alpha\text{-H}_b$), 2.46–2.36 (m, 1H; Pea2-H), 2.36 (dd, $^3J = 6.3$ Hz, $^2J = 13.9$ Hz, 1H; Pea3- H_{ax}), 2.03 (dd, $^3J = 7.6$ Hz, $^2J = 13.7$ Hz, 1H; Pea3- H_{eq}), 1.99–1.86 (m, 1H; Hex4- H_a), 1.68 (s, 3H; Pea7- H_3), 1.52–1.40 (m, 1H; Hex3- H_a), 1.29–1.16 (m, 4H; Hex3- H_b , TIPS), 1.11 (d, $^3J = 6.1$ Hz, 3H; Hex1- H_3), 1.08 (d, $^3J = 7.2$ Hz, 18H; TIPS), 1.10–1.06 (m, 3H; Pea6- H_3), 0.95 (d, $^3J = 6.8$ Hz, 3H; Ala $\beta\text{-H}_3$) ppm; ^{13}C NMR (100 MHz, CDCl_3): δ 176.0 (Pea-1), 173.9 (Ala-C=O), 170.4 (Trp-C=O), 168.9 ($\beta\text{Tyr-C=O}$), 155.4 ($\beta\text{Tyr-4}$), 142.8 (Pea-4), 137.6 (Hex-5), 136.0 (Trp-7a), 132.9 ($\beta\text{Tyr-1}$), 127.5 ($2 \times$, $\beta\text{Tyr-2}$, $\beta\text{Tyr-6}$), 127.3 (Trp-3a), 122.0 ($2 \times$, Trp-2, Trp-6), 119.7 ($2 \times$, $\beta\text{Tyr-3}$, $\beta\text{Tyr-5}$), 119.4 (Trp-5), 118.5 (Trp-4), 114.9 (Hex-6), 112.4 (Pea-5), 111.1 (Trp- β), 111.0 (Trp-7), 70.7 (Hex-2), 56.8 (Trp- α), 49.4 ($\beta\text{Tyr-}\beta$), 45.7 (Ala- α), 41.7 (Pea-3), 40.8 ($\beta\text{Tyr-}\alpha$), 38.7 (Pea-2), 34.8 (Hex-3), 31.0 (Trp-NCH $_3$), 29.4 (Hex-4), 23.3 (Trp- β), 22.2 (Pea-7), 19.8 (Hex-1), 17.9 ($6 \times$, TIPS), 17.2 (Ala- β), 16.9 (Pea-6), 12.6 ($3 \times$, TIPS) ppm; IR (neat): $\tilde{\nu} = 3306, 3062, 2942, 2867, 1731, 1639, 1510$ cm^{-1} ; HR-MS (ESI): calcd for $\text{C}_{46}\text{H}_{69}\text{N}_4\text{O}_6\text{Si}$ [$\text{M} + \text{H}$] $^+$: 801.4981, found 801.4989.

Synthesis of Chondramide C Analogues E-28a, Z-28a, E-29a, and Z-29a. Peptide diene **23b** (26 mg, 34 μmol - see Supporting Information for details of synthesis) was placed in an oven-dried 100 mL two-neck flask equipped with a stirring bar and dissolved in PhMe (30 mL, 1.0 mM). Argon was bubbled through the colorless solution *via* canula at 23 $^\circ\text{C}$ for 10 min. A condenser was then placed on one neck, the flask was placed in an oil bath at 110 $^\circ\text{C}$, and argon bubbling was continued for a further 10 min. Grubbs’ second-generation catalyst (**25**) (7 mg, 8.5 μmol , 25 mol %) was dissolved in PhMe (1 mL), and the dark-red solution was added rapidly *via* syringe to the diene solution. The resulting dark solution was stirred for 2 h at 110 $^\circ\text{C}$ oil bath temperature with continuous argon purging, after which the solution was cooled down to 23 $^\circ\text{C}$ and concentrated to yield the crude product. Two successive column chromatographies (i) 50% AcOEt in cyclohexane, (ii) 33% AcOEt in cyclohexane) of the crude material yielded *cyclo*-[Ala-D-MeTrp- βTyr (OTBS)-(2R,4E,6S,7R)-Hto] **E-28a** (4.4 mg, 6.0 μmol , 18%) and *cyclo*-[Ala-D-MeTrp- βTyr (OTBS)-(2R,4Z,6S,7R)-Hto] **Z-28a** (6.4 mg, 8.8 μmol , 26%) as colorless waxes.

cyclo-[Ala-D-MeTrp- βTyr (OTBS)-(2R,4E,6S,7R)-Hto] **E-28a**. $R_f = 0.16$ (cyclohexane/AcOEt 1:2); LC: $t_R = 11.76$ min (Method C - see Supporting Information); $[\alpha]_D = +38.2$ ($c = 0.90$ in CHCl_3); ^1H NMR (400 MHz, CDCl_3): δ 8.00 (s, 1H; Trp2-NH), 7.58 (d, $^3J = 7.9$ Hz, 1H; Trp4-H), 7.31 (d, $^3J = 8.0$ Hz, 1H; Trp7-H), 7.18 (ddd, $^4J = 1.2$ Hz, $^3J = 8.1/7.1$ Hz, 1H; Trp6-H), 7.12 (ddd, $^4J = 1.1$ Hz, $^3J = 7.9/7.1$ Hz, 1H; Trp5-H), 6.99 (d, $^3J = 8.5$ Hz, 2H; $\beta\text{Tyr}2\text{-H}$),

H, β Tyr6-*H*), 6.91 (d, $^3J = 2.3$ Hz, 1H; Trp2-*H*), 6.72 (d, $^3J = 8.6$ Hz, 2H; β Tyr3-*H*, β Tyr5-*H*), 6.54 (d, $^3J = 6.6$ Hz, 1H; Ala α -NH), 6.36 (d, $^3J = 9.2$ Hz, 1H; β Tyr β -NH), 5.49 (dd, $^3J = 9.5/7.0$ Hz, 1H; Trp α -*H*), 5.48–5.41 (m, 1H; β Tyr β -*H*), 5.08 (d, $^3J = 10.1$ Hz, 1H; Hto5-*H*), 4.79 (dq, $^3J = 6.1/2.9$ Hz, 1H; Hto7-*H*), 4.64 (dq, $^3J = 6.7/6.7$ Hz, 1H; Ala α -*H*), 3.29 (dd, $^3J = 7.1$ Hz, $^2J = 15.3$ Hz, 1H; Trp β -*H*_a), 3.21 (dd, $^3J = 9.6$ Hz, $^2J = 15.4$ Hz, 1H; Trp β -*H*_b), 2.91 (s, 3H; Trp-NCH₃), 2.72–2.64 (m, 3H; β Tyr α -*H*₂, Hto6-*H*), 2.38 (dq, $^3J = 9.8/7.0/2.8$ Hz, 1H; Hto2-*H*), 2.28 (dd, $^3J = 4.5$ Hz, $^2J = 13.4$ Hz, 1H; Hto3-*H*_a), 2.08 (dd, $^3J = 13.1$ Hz, $^2J = 13.1$ Hz, 1H; Hto3-*H*_b), 1.60 (s, 3H; Hto10-*H*₃), 1.20 (d, $^3J = 7.1$ Hz, 3H; Ala β -*H*₃), 0.98 (s, 9H; TBS), 0.94 (d, $^3J = 6.2$ Hz, 3H; Hto9-*H*₃), 0.82 (d, $^3J = 5.4$ Hz, 3H; Hto11-*H*₃), 0.81 (d, $^3J = 5.3$ Hz, 3H; Hto8-*H*₃), 0.19 (d, $^3J = 0.7$ Hz, 6H; TBS) ppm; ^{13}C NMR (100 MHz, CDCl₃): δ 174.1 (Hto-1), 174.0 (Ala-C=O), 170.9 (β Tyr-C=O), 168.8 (Trp-C=O), 154.9 (β Tyr-4), 136.1 (Trp-7a), 133.9 (Hto-4/ β Tyr-1), 133.8 (β Tyr-1/Hto-4), 127.1 (Trp-3a), 126.8 (2 \times , β Tyr-2, β Tyr-6), 126.5 (Hto-5), 122.2 (Trp-2/Trp-6), 122.2 (Trp-6/Trp-2), 120.1 (2 \times , β Tyr-3, β Tyr-5), 119.6 (Trp-5), 118.4 (Trp-4), 111.1 (Trp-7), 110.5 (Trp-3), 75.0 (Hto-7), 56.4 (Trp- α), 50.0 (β Tyr- β), 46.7 (Ala- α), 45.7 (Hto-3), 41.7 (β Tyr- α), 41.4 (Hto-2), 37.0 (Hto-6), 30.1 (Trp-NCH₃), 25.6 (3 \times , TBS), 23.7 (Trp- β), 19.2 (Ala- β), 18.4 (Hto-9), 18.2 (Hto-11), 18.2 (TBS), 17.7 (Hto-8), 15.0 (Hto-10), -4.4 (2 \times , TBS) ppm; IR (neat): $\tilde{\nu} = 3320$, 2958, 2930, 1722, 1671, 1635, 1459, 1263, 1207, 914, 840, 804, 782, 741 cm⁻¹; HR-MS (ESI): calcd for C₄₁H₅₉N₄O₆Si [M + H]⁺: 731.4198, found 731.4202.

cyclo-[Ala-D-MeTrp- β Tyr(OTBS)-(2R,4Z,6S,7R)-Hto] Z-28a. *R*_f = 0.39 (cyclohexane/AcOEt 1:2); LC: *t*_R = 11.99 min (Method C - see Supporting Information); [α]_D = +9.1 (*c* = 0.90 in CHCl₃); ^1H NMR (500 MHz, CDCl₃): δ 7.97 (s, 1H; Trp2-NH), 7.58 (d, $^3J = 7.9$ Hz, 1H; Trp4-*H*), 7.33 (d, $^3J = 8.1$ Hz, 1H; Trp7-*H*), 7.19–7.13 (m, 2H; β Tyr β -NH, Trp6-*H*), 7.12 (t, $^3J = 7.5$ Hz, 1H; Trp5-*H*), 6.94 (d, $^3J = 8.5$ Hz, 2H; β Tyr2-*H*, β Tyr6-*H*), 6.83 (d, $^3J = 6.6$ Hz, 1H; Ala α -NH), 6.78 (d, $^3J = 1.9$ Hz, 1H; Trp2-*H*), 6.70 (d, $^3J = 8.6$ Hz, 2H; β Tyr3-*H*, β Tyr5-*H*), 5.44 (dd, $^3J = 8.2/8.2$ Hz, 1H; Trp α -*H*), 5.23 (dd, $^3J = 8.9/3.4$ Hz, 1H; β Tyr β -*H*), 4.87 (d, $^3J = 8.9$ Hz, 1H; Hto5-*H*), 4.75–4.65 (m, 2H; Hto7-*H*, Ala α -*H*), 3.33 (dd, $^3J = 7.9$ Hz, $^2J = 15.3$ Hz, 1H; Trp β -*H*_a), 3.17 (dd, $^3J = 8.5$ Hz, $^2J = 15.1$ Hz, 1H; Trp β -*H*_b), 2.98 (s, 3H; Trp-NCH₃), 2.77–2.71 (m, 1H; Hto6-*H*), 2.70 (dd, $^3J = 3.4$ Hz, $^2J = 15.1$ Hz, 1H; β Tyr α -*H*_a), 2.67–2.53 (m, 3H; β Tyr α -*H*_b, Hto2-*H*, Hto3-*H*_a), 2.11–2.03 (m, 1H; Hto3-*H*_b), 1.71 (s, 3H; Hto10-*H*₃), 1.21 (d, $^3J = 6.6$ Hz, 3H; Ala β -*H*₃), 1.15 (d, $^3J = 6.6$ Hz, 3H; Hto9-*H*₃), 1.02 (d, $^3J = 6.6$ Hz, 3H; Hto11-*H*₃), 0.98 (s, 9H; TBS), 0.79 (d, $^3J = 6.8$ Hz, 3H; Hto8-*H*₃), 0.19 (s, 6H; TBS) ppm; ^{13}C NMR (100 MHz, CDCl₃): δ 174.8 (Hto-1), 173.6 (Ala-C=O), 170.3 (β Tyr-C=O), 168.8 (Trp-C=O), 154.8 (β Tyr-4), 136.0 (Trp-7a), 135.1 (Hto-4), 133.6 (β Tyr-1), 128.6 (Hto-5), 127.1 (Trp-3a), 127.0 (2 \times , β Tyr-2, β Tyr-6), 122.2 (Trp-2/Trp-6), 122.1 (Trp-6/Trp-2), 119.9 (2 \times , β Tyr-3, β Tyr-5), 119.5 (Trp-5), 118.4 (Trp-4), 111.0 (Trp-7), 110.4 (Trp-3), 74.1 (Hto-7), 56.1 (Trp- α), 49.6 (β Tyr- β), 45.9 (Ala- α), 41.5 (β Tyr- α), 40.2 (Hto-2), 37.8 (Hto-3), 34.0 (Hto-6), 30.1 (Trp-NCH₃), 25.6 (3 \times , TBS), 23.4 (Trp- β), 22.8 (Ala- β), 18.4 (Hto-9), 18.2 (TBS), 16.9 (Hto-11), 12.7 (Hto-10), 12.5 (Hto-8), -4.3 (2 \times , TBS) ppm; IR (neat): $\tilde{\nu} = 3325$, 2932, 1678, 1632, 1510, 1460, 1261, 1205, 1173, 1066, 913, 840, 804, 782, 740 cm⁻¹; HR-MS (ESI): calcd for C₄₁H₅₉N₄O₆Si [M + H]⁺: 731.4198, found 731.4201.

cyclo-[Ala-D-MeTrp- β Tyr-(2R,4E,6S,7R)-Hto] E-29a. To a solution of **E-28a** (11 mg, 15 μ mol) in THF (0.75 mL, 20 mM) in a 5 mL round-bottomed flask was added at 23 °C by micropipet TBAF (1.0 equiv, 15 μ mol) as a solution in THF (1.0 M, 15 μ L). The reaction was stirred for 30 min, and then all solvents were removed by reduced pressure. Purification of the crude material by column chromatography (67% cyclohexane in AcOEt, then 3% MeOH in CH₂Cl₂) yielded **E-29a** as a colorless wax (7.1 mg, 12 μ mol, 77%, 14% over two steps) that was further purified by preparative HPLC (Method E - see Supporting Information) prior to cytotoxicity studies to yield a colorless powder after lyophilization.

*R*_f = 0.10 (CH₂Cl₂/MeOH 25:1); LC: *t*_R = 8.51 min (Method C - see Supporting Information); [α]_D = +26.5 (*c* = 0.60 in MeOH); ^1H NMR (500 MHz, [*d*₆]DMSO): δ 10.76 (s, 1H; Trp2-NH), 9.27 (br s, 1H; β Tyr4-OH), 8.38 (d, $^3J = 9.1$ Hz, 1H; β Tyr β -NH), 7.54 (d, $^3J = 7.9$ Hz, 1H; Trp4-*H*), 7.29 (d, $^3J = 8.1$ Hz, 1H; Trp7-*H*), 7.10–7.00 (m, 4H; Trp6-*H*, β Tyr2-*H*, β Tyr6-*H*, Trp2-*H*), 6.95 (t, $^3J = 7.3$ Hz, 1H; Trp5-*H*), 6.85 (d, $^3J = 6.7$ Hz, 1H; Ala α -NH), 6.66 (d, $^3J = 8.5$ Hz, 2H; β Tyr3-*H*, β Tyr5-*H*), 5.52 (dd, $^3J = 9.6/6.4$ Hz, 1H; Trp α -*H*), 5.19 (t, $^3J = 10.4$ Hz, β Tyr β -*H*), 5.00 (d, $^3J = 9.7$ Hz, 1H; Hto5-*H*), 4.67 (dd, $^3J = 6.2/3.0$ Hz, 1H; Hto7-*H*), 4.47 (dq, $^3J = 6.7/6.7$ Hz, 1H; Ala α -*H*), 3.05 (dd, $^3J = 9.9$ Hz, $^2J = 15.0$ Hz, 1H; Trp β -*H*_a), 2.97 (dd, $^3J = 6.0$ Hz, $^2J = 15.0$ Hz, 1H; Trp β -*H*_b), 2.91 (s, 3H; Trp-NCH₃), 2.76 (dd, $^3J = 11.5$ Hz, $^2J = 13.4$ Hz, 1H; β Tyr α -*H*_a), 2.56 (dd, $^3J = 2.3$ Hz, $^2J = 13.4$ Hz, 1H; β Tyr α -*H*_b), 2.52–2.46 (m, 1H; Hto2-*H*), 2.44–2.34 (m, 1H; Hto6-*H*), 2.15 (app d, $^2J = 13.4$ Hz, 1H; Hto3-*H*_a), 2.00 (dd, $^3J = 12.8$ Hz, $^2J = 12.8$ Hz, 1H; Hto3-*H*_b), 1.53 (s, 3H; Hto10-*H*₃), 1.10 (d, $^3J = 7.1$ Hz, 3H; Hto9-*H*₃), 0.83 (d, $^3J = 6.2$ Hz, 3H; Hto11-*H*₃), 0.80 (d, $^3J = 6.9$ Hz, 3H; Hto8-*H*₃), 0.71 (d, $^3J = 6.7$ Hz, 3H; Ala β -*H*₃) ppm; ^{13}C NMR (125 MHz, CDCl₃): δ 172.7 (Hto-1), 171.9 (Ala-C=O), 171.2 (β Tyr-C=O), 168.4 (Trp-C=O), 156.0 (β Tyr-4), 135.9 (Trp-7a), 133.2 (Hto-4), 132.1 (β Tyr-1), 127.1 (2 \times , β Tyr-2, β Tyr-6), 126.9 (Trp-3a), 125.9 (Hto-5), 123.1 (Trp-2), 120.7 (Trp-6), 118.2 (Trp-5), 118.0 (Trp-4), 114.8 (2 \times , β Tyr-3, β Tyr-5), 111.0 (Trp-7), 109.0 (Trp-3), 73.8 (Hto-7), 54.8 (Trp- α), 49.5 (β Tyr- β), 45.4 (Ala- α), 44.4 (Hto-3), 41.3 (β Tyr- α), 40.6 (Hto-2), 36.0 (Hto-6), 29.5 (Trp-NCH₃), 24.1 (Trp- β), 18.4 (Ala- β), 17.5 (Hto-9), 17.5 (Hto-11), 17.3 (Hto-10), 14.8 (Hto-8) ppm; HR-MS (ESI): calcd for C₃₅H₄₅N₄O₆ [M + H]⁺: 617.3334, found 617.3332.

cyclo-[Ala-D-MeTrp- β Tyr-(2R,4Z,6S,7R)-Hto] Z-29a. The desilylation of **Z-28a** (11 mg, 15 μ mol) was performed according to the procedure described for the desilylation of **E-28a**. Purification of the crude material by column chromatography (67% cyclohexane in AcOEt, then 3% MeOH in CH₂Cl₂) yielded **Z-29a** as a colorless wax (7.8 mg, 13 μ mol, 88%, 23% over two steps), which was purified further by preparative HPLC (Method E - see Supporting Information) prior to cytotoxicity studies to yield a colorless powder after lyophilization.

*R*_f = 0.17 (CH₂Cl₂/MeOH 25:1); LC: *t*_R = 8.80 min (Method C - see Supporting Information); [α]_D = +3.2 (*c* = 0.60 in MeOH); ^1H NMR (500 MHz, [*d*₆]DMSO): δ 10.81 (s, 1H; Trp2-NH), 9.25 (s, 1H; β Tyr4-OH), 8.60 (d, $^3J = 8.3$ Hz, 1H; β Tyr β -NH), 7.56 (d, $^3J = 7.9$ Hz, 1H; Trp4-*H*), 7.31 (d, $^3J = 8.1$ Hz, 1H; Trp7-*H*), 7.11–6.99 (m, 4H; Trp6-*H*, β Tyr2-*H*, β Tyr6-*H*, Trp2-*H*), 6.97 (t, $^3J = 7.4$ Hz, 1H; Trp5-*H*), 6.85 (d, $^3J = 6.7$ Hz, 1H; Ala α -NH), 6.66 (d, $^3J = 8.5$ Hz, 2H; β Tyr3-*H*, β Tyr5-*H*), 5.44 (dd, $^3J = 9.2/6.8$ Hz, 1H; Trp α -*H*), 5.15–5.06 (m, 1H; β Tyr β -*H*), 4.83 (d, $^3J = 9.7$ Hz, 1H; Hto5-*H*), 4.64 (dq, $^3J = 6.5/4.3$ Hz, 1H; Hto7-*H*), 4.51 (dq, $^3J = 6.6/6.6$ Hz, 1H; Ala α -*H*), 3.07 (dd, $^3J = 9.4$ Hz, $^2J = 15.3$ Hz, 1H; Trp β -*H*_a), 2.98 (s, 3H; Trp-NCH₃), 2.96 (dd, $^3J = 6.3$ Hz, $^2J = 15.1$ Hz, 1H; Trp β -*H*_b), 2.69–2.62 (m, 2H; β Tyr α -*H*₂), 2.59–2.52 (m, 1H; Hto2-*H*), 2.48–2.35 (m, 2H; Hto6-*H*, Hto3-*H*_a), 1.94 (dd, $^3J = 4.1$ Hz, $^2J = 12.7$ Hz, 1H; Hto3-*H*_b), 1.66 (s, 3H; Hto10-*H*₃), 1.11 (d, $^3J = 6.7$ Hz, 3H; Ala β -*H*₃), 1.02 (d, $^3J = 6.6$ Hz, 3H; Hto9-*H*₃), 0.89 (d, $^3J = 6.6$ Hz, 3H; Hto11-*H*₃), 0.68 (d, $^3J = 6.8$ Hz, 3H; Hto8-*H*₃) ppm; ^{13}C NMR (125 MHz, [*d*₆]DMSO): δ 172.6 (Hto-1), 172.0 (Ala-C=O), 168.9 (β Tyr-C=O), 168.5 (Trp-C=O), 155.9 (β Tyr-4), 136.0 (Trp-7a), 133.7 (Hto-4), 132.5 (β Tyr-1), 128.0 (Hto-5), 126.9 (2 \times , β Tyr-2, β Tyr-6), 126.8 (Trp-3a), 122.7 (Trp-2), 120.8 (Trp-6), 118.1 (Trp-5), 118.0 (Trp-4), 114.8 (2 \times , β Tyr-3, β Tyr-5), 111.0 (Trp-7), 109.1 (Trp-3), 72.2 (Hto-7), 54.8 (Trp- α), 48.9 (β Tyr- β), 44.8 (Ala- α), 44.4 (Hto-3), 41.8 (β Tyr- α), 40.0 (Hto-2), 37.7 (Hto-6), 33.8 (Trp-NCH₃), 24.0 (Trp- β), 22.7 (Ala- β), 17.8 (Hto-9), 17.6 (Hto-11), 12.8 (Hto-10), 12.5 (Hto-8) ppm; HR-MS (ESI): calcd for C₃₅H₄₅N₄O₆ [M + H]⁺: 617.3334, found 617.3331.

Synthesis of Simplified Jasplakinolide/Jaspamide Analogues E-30c and E-31c. **cyclo-[Ala-D-MeTrp- β Tyr-(2S,4E,8S)-Htn] (E-31c).** **Conditions A.** Peptide diene **23n** (29 mg, 36 μ mol) was subjected to RCM according to the conditions described for the

RRCM of peptide diene **23b**. Column chromatography (70% AcOEt in cyclohexane) of the crude metathesis product yielded *E*-**30c** (16.9 mg, 21.9 μ mol, 61%) as a pale brown wax.

Conditions B. Peptide diene **23n** (6.8 mg, 8.5 μ mol) was placed in an oven-dried microwave tube equipped with a stirring bar and dissolved in anhydrous CH_2Cl_2 (6.0 mL). Catalyst **25** (0.36 mg, 0.043 μ mol, 10 mol %) was dissolved separately in anhydrous CH_2Cl_2 (2.5 mL) and the red solution introduced rapidly to the reaction via plastic syringe (total volume = 8.5 mL, 1 mM). The vessel was then hermetically sealed and heated in an oil bath (40 °C) with stirring for 2 h. The reaction was then cooled and the solvent removed under reduced pressure. Column chromatography (70% AcOEt in cyclohexane) of the crude metathesis product yielded *cyclo*-[Ala-D-MeTrp- β Tyr(OTIPS)-(2*S*,4*E*,8*S*)-Htn] *E*-**30c** (4.3 mg, 5.5 μ mol, 65%) as a pale brown wax.

cyclo-[Ala-D-MeTrp- β Tyr(OTIPS)-(2*S*,4*E*,8*S*)-Htn] *E*-**30c**. R_f = 0.26 (AcOEt/cyclohexane 7:3); LC: t_R = 12.20 min (Method B - see Supporting Information); $[\alpha]_D^{20}$ = +32.5 (c = 0.08 in CHCl_3); ^1H NMR (400 MHz, CDCl_3): δ 8.09 (s, 1H; Trp2-NH), 7.62 (d, 3J = 7.8 Hz, 1H; Trp4-H), 7.33 (d, 3J = 8.0 Hz, 1H; Trp7-H), 7.18 (td, 4J = 1.0 Hz, 3J = 7.1 Hz, 1H; Trp6-H), 7.16–7.10 (m, 1H; β Tyr β -NH), 7.12 (td, 3J = 7.1 Hz, 1H; Trp5-H), 7.04 (d, 3J = 8.4 Hz, 2H; β Tyr2-H, β Tyr6-H), 6.94 (s, 1H; Trp2-H), 6.80 (d, 3J = 8.2 Hz, 2H; β Tyr3-H, β Tyr5-H), 6.69–6.67 (m, 1H; Ala α -NH), 5.68 (dd, 3J = 8.8/7.3 Hz, 1H; Trp α -H), 5.24 (ddd, 3J = 8.3/8.3/3.8 Hz, 1H; β Tyr β -H), 5.03 (t, 3J = 6.8 Hz, 1H; Htn5-H), 4.85–4.74 (m, 2H; Htn8-H, Ala α -H), 3.38 (dd, 3J = 7.0 Hz, 2J = 15.6 Hz, 1H; Trp β -H_a), 3.23 (dd, 3J = 9.3 Hz, 2J = 15.4 Hz, 1H; Trp β -H_b), 2.92 (s, 3H; Trp-NCH₃), 2.78 (dd, 3J = 3.9 Hz, 2J = 15.1 Hz, 1H; β Tyr α -H_a), 2.58 (dd, 3J = 8.6 Hz, 2J = 15.1 Hz, 1H; β Tyr α -H_b), 2.45–2.40 (m, 2H; Htn2-H, Htn3-H_a), 1.90–1.80 (m, 3H; Htn3-H_b, Htn6-H₂), 1.59–1.51 (m, 1H; Htn7-H_a), 1.50 (s, 3H; Htn11-H₃), 1.39–1.30 (m, 1H; Htn7-H_b), 1.30–1.16 (m, 6H; Htn10-H₃ and TIPS), 1.10 (d, 3J = 7.4 Hz, 18H; TIPS), 1.08 (d, 3J = 6.2 Hz, 3H; Htn9-H₃), 0.97 (d, 3J = 6.8 Hz, 3H; Ala β -H₃) ppm; ^{13}C NMR (100 MHz, CDCl_3): δ 174.7, 174.3, 170.3, 169.0, 155.4, 136.2, 134.0, 132.8, 127.3, 127.0, 124.4, 122.1, 121.9, 119.9, 119.8, 119.5, 118.6, 111.1, 111.0, 69.8, 55.8, 48.9, 46.0, 43.4, 39.8, 39.7, 35.5, 30.2, 29.6, 23.2, 22.9, 20.2, 19.8, 18.0, 17.9, 16.3, 12.6 ppm; IR (thin film): $\tilde{\nu}$ = 3310, 2927, 2867, 1730, 1660, 1636, 1509 cm^{-1} ; HR-MS (ESI): calcd for $\text{C}_{44}\text{H}_{65}\text{N}_4\text{O}_6\text{Si}$ [M + H]⁺: 773.4673, found 773.4673; calcd for $\text{C}_{44}\text{H}_{64}\text{N}_4\text{NaO}_6\text{Si}$ [M + Na]⁺: 795.4493, found 795.4484.

cyclo-[Ala-D-MeTrp- β Tyr-(2*S*,4*E*,8*S*)-Htn] (*E*-**31c**). The desilylation of *E*-**30c** (13 mg, 17 μ mol) was performed according to the procedure described for the desilylation of *E*-**28a**. Column chromatography (AcOEt/cyclohexane) of the crude material yielded *E*-**31c** as a colorless wax (10 mg, 16 μ mol, 97%, 58% over two steps), which was purified again prior to cytotoxicity studies by preparative HPLC (Method E - see Supporting Information) to afford a colorless powder after lyophilization.

R_f = 0.31 (AcOEt/cyclohexane 4:1); LC: t_R = 7.13 min (Method A - see Supporting Information); $[\alpha]_D$ = +36.9 (c = 0.79 in MeOH); ^1H NMR (500 MHz, CDCl_3): δ 8.29 (s, 1H; Trp2-NH),

7.60 (d, 3J = 7.9 Hz, 1H; Trp4-H), 7.32 (d, 3J = 8.0 Hz, 1H; Trp7-H), 7.22 (d, 3J = 8.2 Hz, 1H; β Tyr β -NH), 7.16 (td, 4J = 1.0 Hz, 3J = 7.2 Hz, 1H; Trp6-H), 7.10 (td, 3J = 7.2 Hz, 1H; Trp5-H), 6.92 (d, 3J = 8.4 Hz, 2H; β Tyr2-H, β Tyr6-H), 6.83 (s, 1H; Trp2-H), 6.71–6.67 (m, 1H; Ala α -NH), 6.68 (d, 3J = 8.2 Hz, 2H; β Tyr3-H, β Tyr5-H), 5.65 (dd, 3J = 8.9/7.2 Hz, 1H; Trp α -H), 5.19 (ddd, 3J = 8.3/8.3/3.9 Hz, 1H; β Tyr β -H), 5.03 (t, 3J = 6.7 Hz, 1H; Htn5-H), 4.85–4.77 (m, 2H; Htn8-H, Ala α -H), 3.42 (dd, 3J = 6.9 Hz, 2J = 15.5 Hz, 1H; Trp β -H_a), 3.16 (dd, 3J = 9.3 Hz, 2J = 15.4 Hz, 1H; Trp β -H_b), 2.96 (s, 3H; Trp-NCH₃), 2.73 (dd, 3J = 3.8 Hz, 2J = 15.5 Hz, 1H; β Tyr α -H_a), 2.54 (dd, 3J = 8.6 Hz, 2J = 15.5 Hz, 1H; β Tyr α -H_b), 2.45–2.40 (m, 2H; Htn2-H, Htn3-H_a), 1.90–1.80 (m, 3H; Htn3-H_b, Htn6-H₂), 1.59–1.51 (m, 1H; Htn7-H_a), 1.48 (s, 3H; Htn11-H₃), 1.39–1.30 (m, 1H; Htn7-H_b), 1.13 (d, 3J = 5.7 Hz, 3H; Htn10-H₃), 1.09 (d, 3J = 6.3 Hz, 3H; Htn9-H₃), 0.99 (d, 3J = 6.7 Hz, 3H; Ala β -H₃) ppm; ^{13}C NMR (150 MHz, CDCl_3): δ = 174.7 (Ala-C=O), 174.7 (Htn-1), 170.5 (Trp-C=O), 169.1 (β Tyr-C=O), 155.7 (β Tyr-4), 136.2 (Trp-7a), 133.9 (Htn-5), 131.9 (β Tyr-1), 127.1 (2 \times , β Tyr-2, β Tyr-6), 127.1 (Trp-3a), 124.5 (Htn-4), 122.1 (Trp-6), 122.0 (Trp-2), 119.4 (Trp-5), 118.5 (Trp-4), 115.6 (2 \times , β Tyr-3, β Tyr-5), 111.2 (Trp-7), 110.4 (Trp-3), 70.0 (Htn-8), 56.2 (Trp- α), 49.2 (β Tyr- β), 46.0 (Ala- α), 43.4 (Htn-7), 40.0 (Htn-2), 40.0 (β Tyr- α), 35.4 (Htn-3), 30.4 (Trp-NCH₃), 23.2 (Htn-6), 23.2 (Trp- β), 20.2 (Htn-9), 19.7 (Htn-10), 18.1 (Ala- β), 16.2 (Htn-11) ppm; IR (neat): $\tilde{\nu}$ = 3308, 3055, 2930, 2854, 1726, 1631, 1510 cm^{-1} ; HR-MS (ESI): calcd for $\text{C}_{35}\text{H}_{45}\text{N}_4\text{O}_6$ [M + H]⁺: 617.3334, found 617.3331.

Acknowledgment. This work was supported by the Max Planck Gesellschaft (to H.W.), the Deutsche Forschungsgemeinschaft (Emmy-Noether young investigator award to H.D.A.), the state of North-Rhine-Westphalia (ZACG Dortmund) and the European Union (RTN Endocyte). T.S.H. and L.G.M. are grateful to the Alexander von Humboldt-Stiftung for research fellowships. We thank Prof. Dr. M. Kalesse for discussions and supply of a sample of natural chondramide C. We also thank Prof. Dr. S. Blechert and Dipl. Chem. D. Rost (TU Berlin) for support and catalyst samples during our metathesis studies, and Dipl. Biol. S. Baumann is thanked for helpful assistance with preparing figure graphics.

Supporting Information Available: Detailed experimental (synthetic and cell screening) procedures, comprehensive compound characterization, including copies of ^1H NMR and ^{13}C NMR spectral data, molecular modeling data, additional graphical representation and numbering convention for peptide diene **23n** and macrocyclic structures *E*-**28a**, *Z*-**28a**, *E*-**29a**, *Z*-**29a**, *E*-**30c**, and *E*-**31c**. This material is available free of charge via the Internet at <http://pubs.acs.org>.

JA9095126